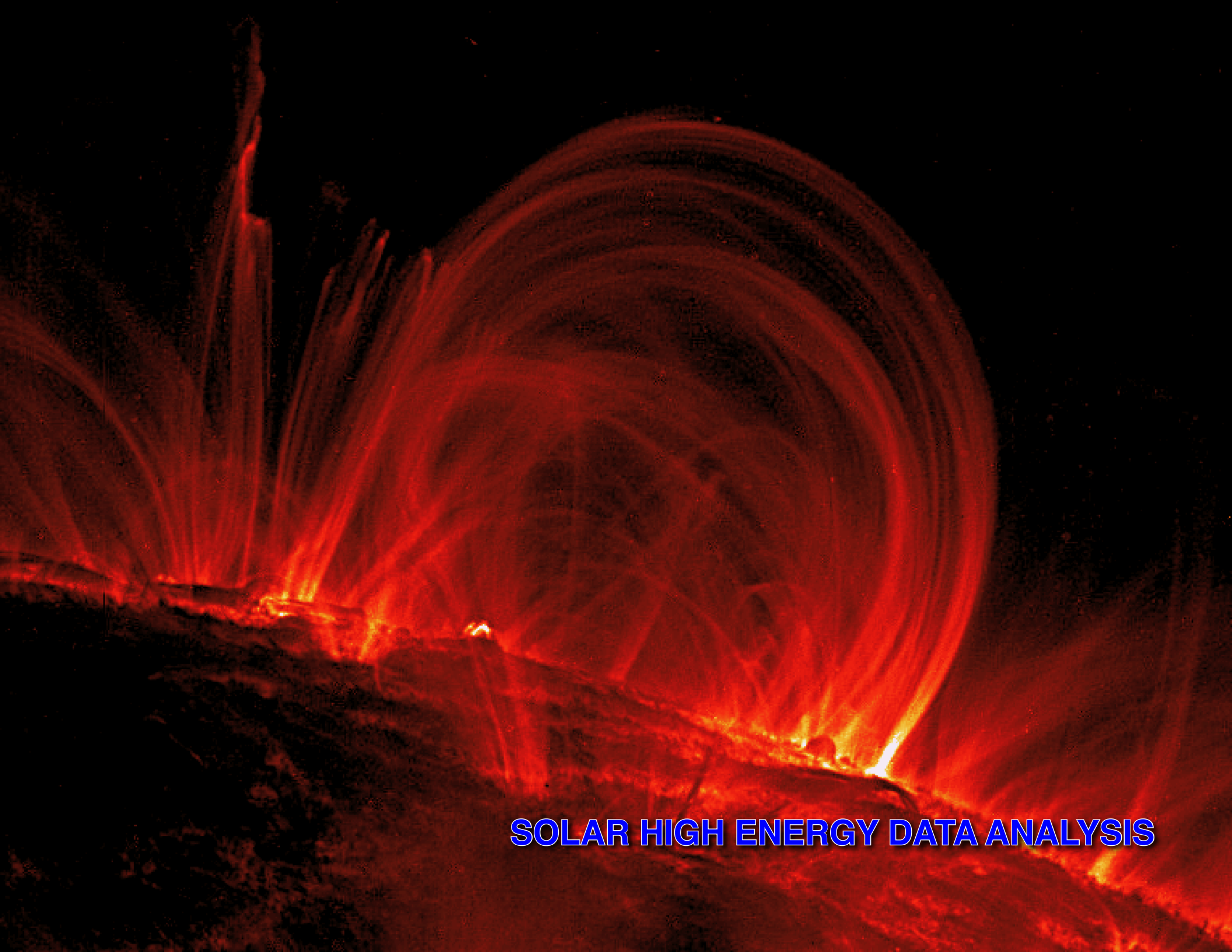
SOLAR HIGH ENERGY DATA ANALYSIS

Overview

- Review of gamma-ray and neutron production
- Examples of data
- Observable quantities
- Transport and interaction model and the parameters
- Dependence of the observable quantities on the parameters
- Data analysis approach
- Analysis of the OSSE/CGRO observations of the 1991 June 4 flare
- Analysis of the RHESSI/Integral/Tsuneb observations of the 2003 October 28 flare

Summary
Nuclear Deexcitation Gamma-Ray Lines

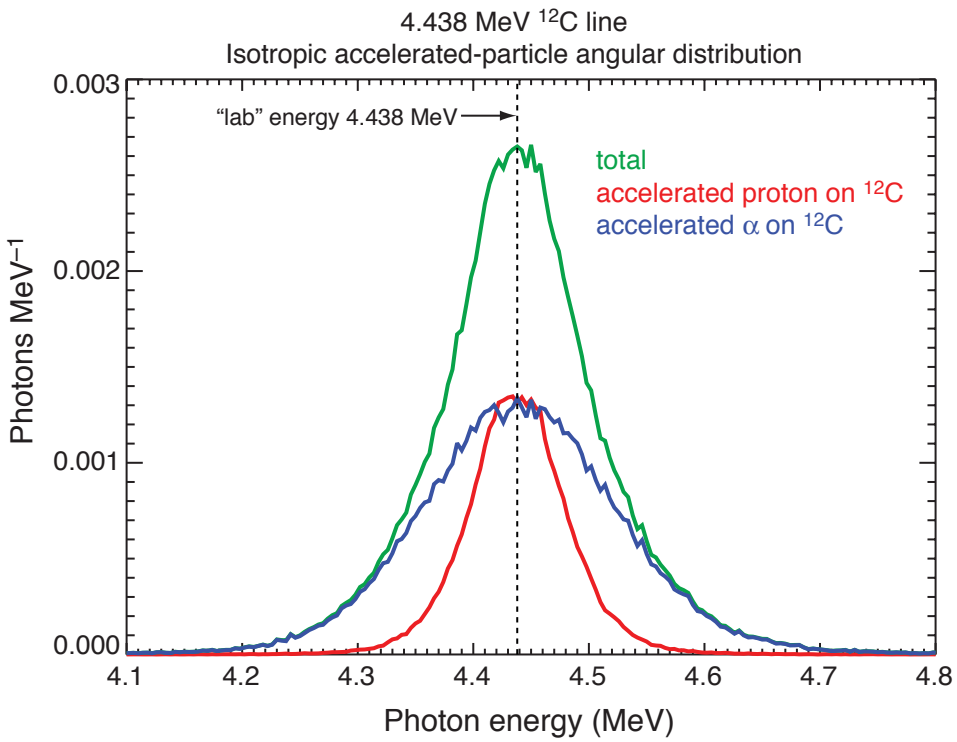

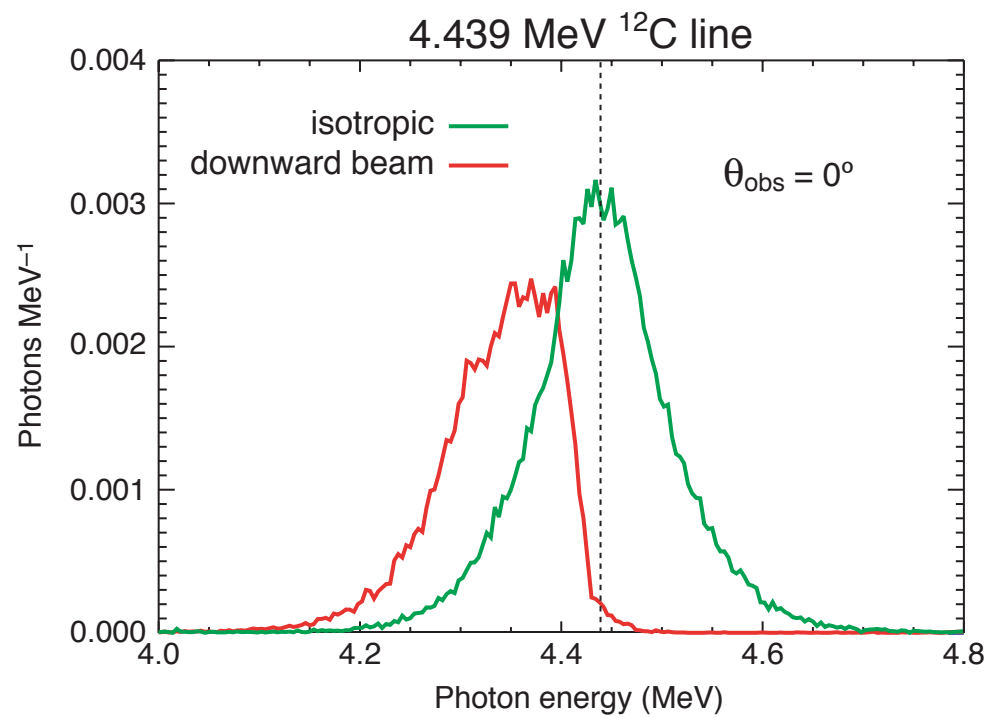

Summary
Positron Annihilation Line

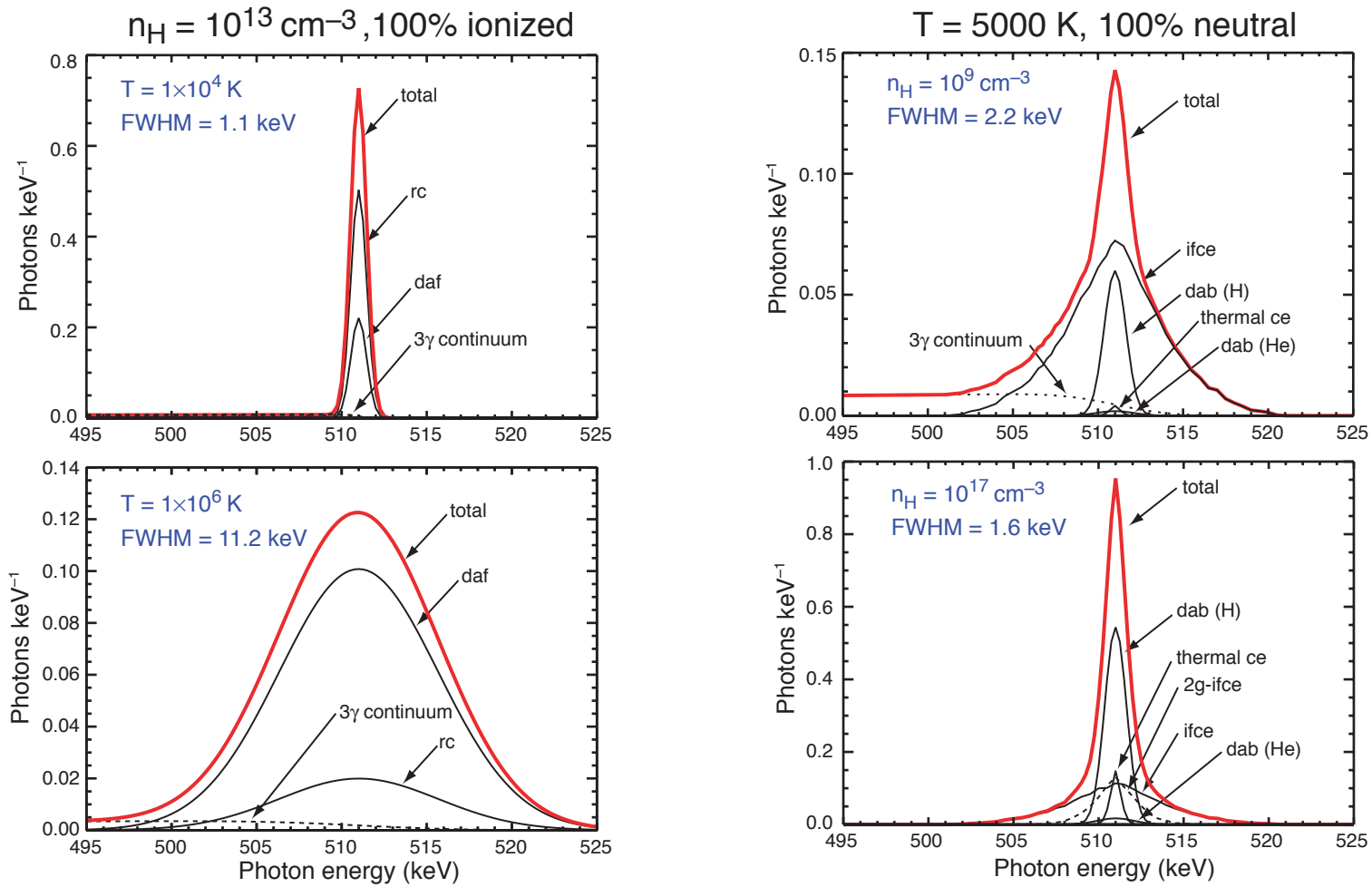

The line shape is NOT Gaussian!

Summary
Escaping Neutron Spectra

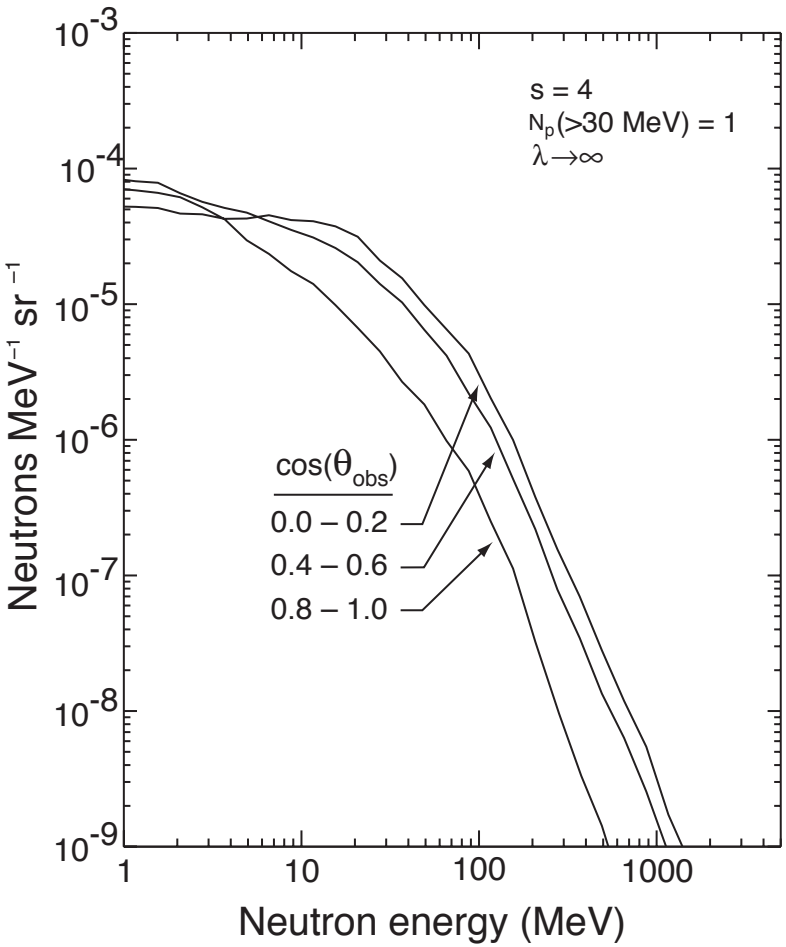

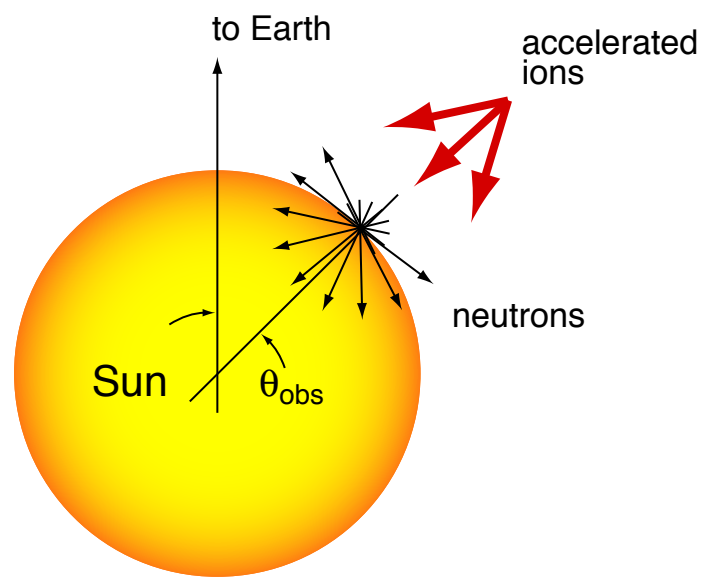

Summary
Neutron Capture Line

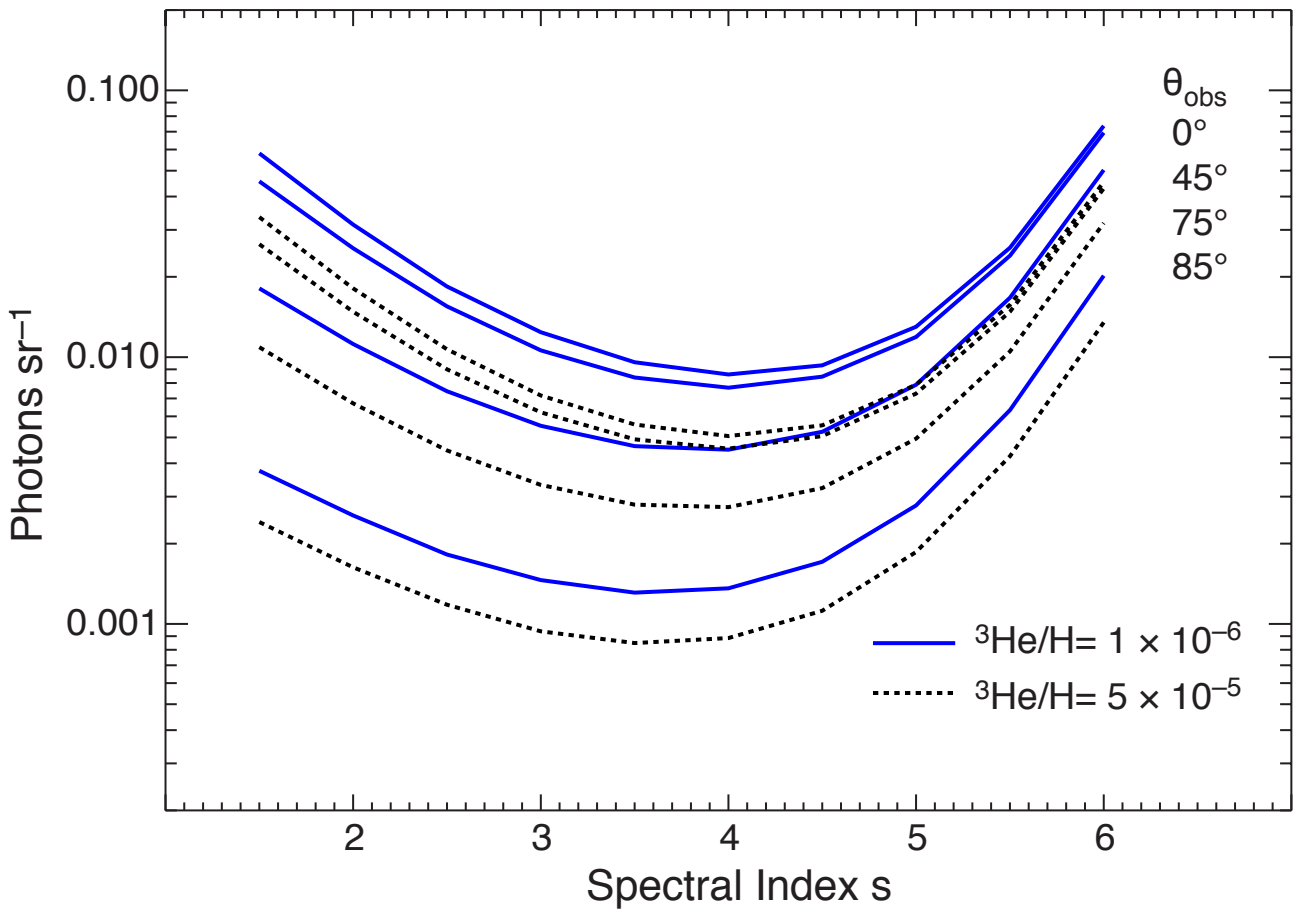

Summary
Pion Decay Emission

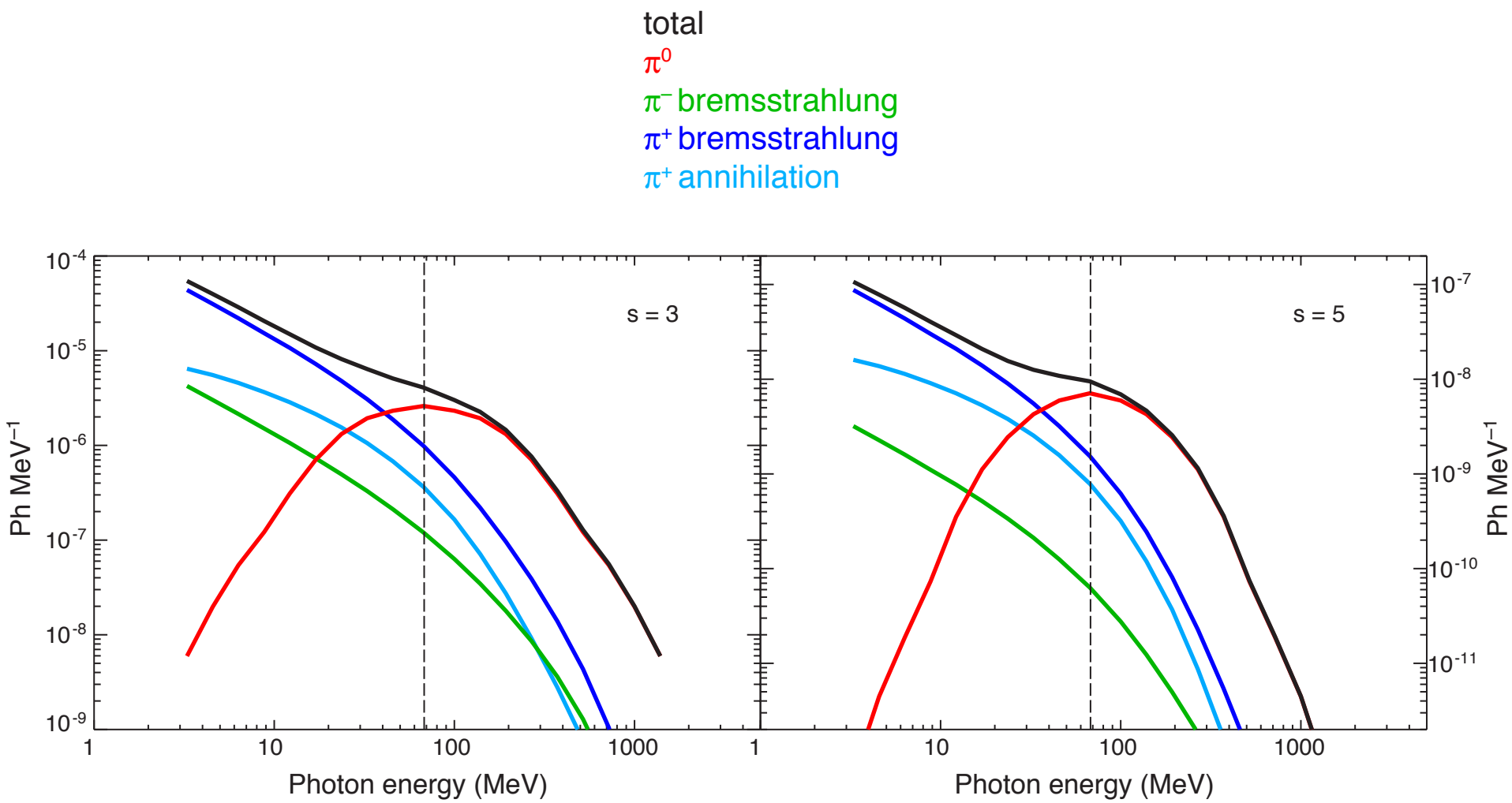

Data Samples
Gamma-ray Count Spectrum

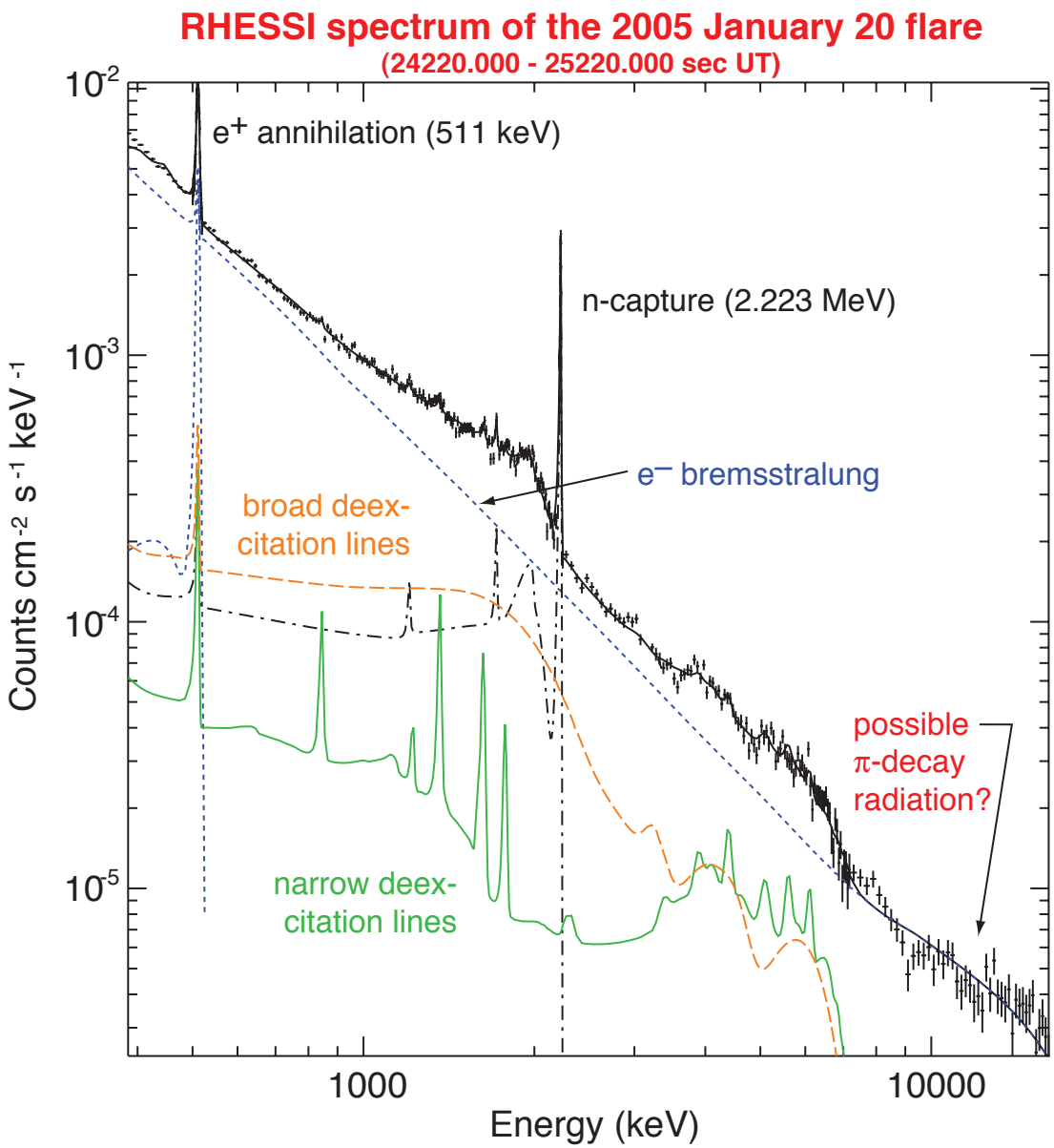

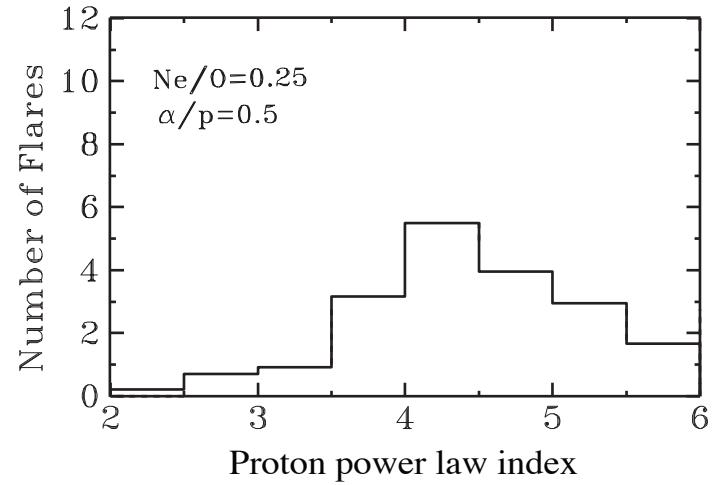

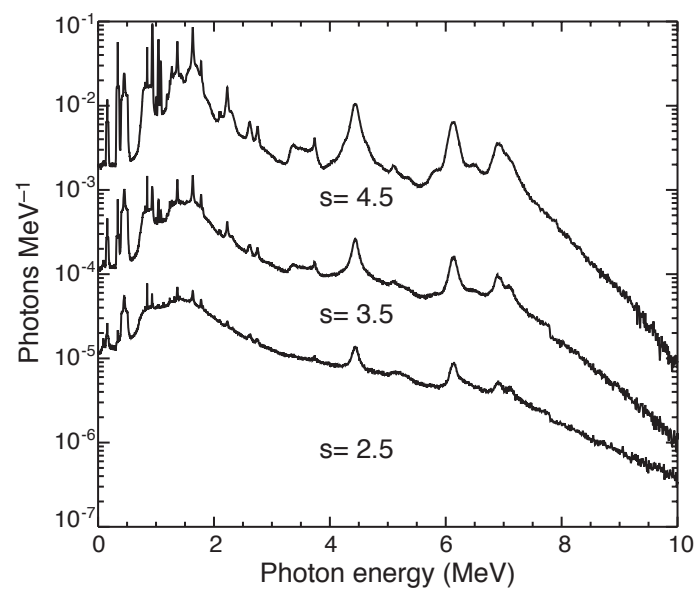

Data Samples
Gamma-ray Count Spectrum

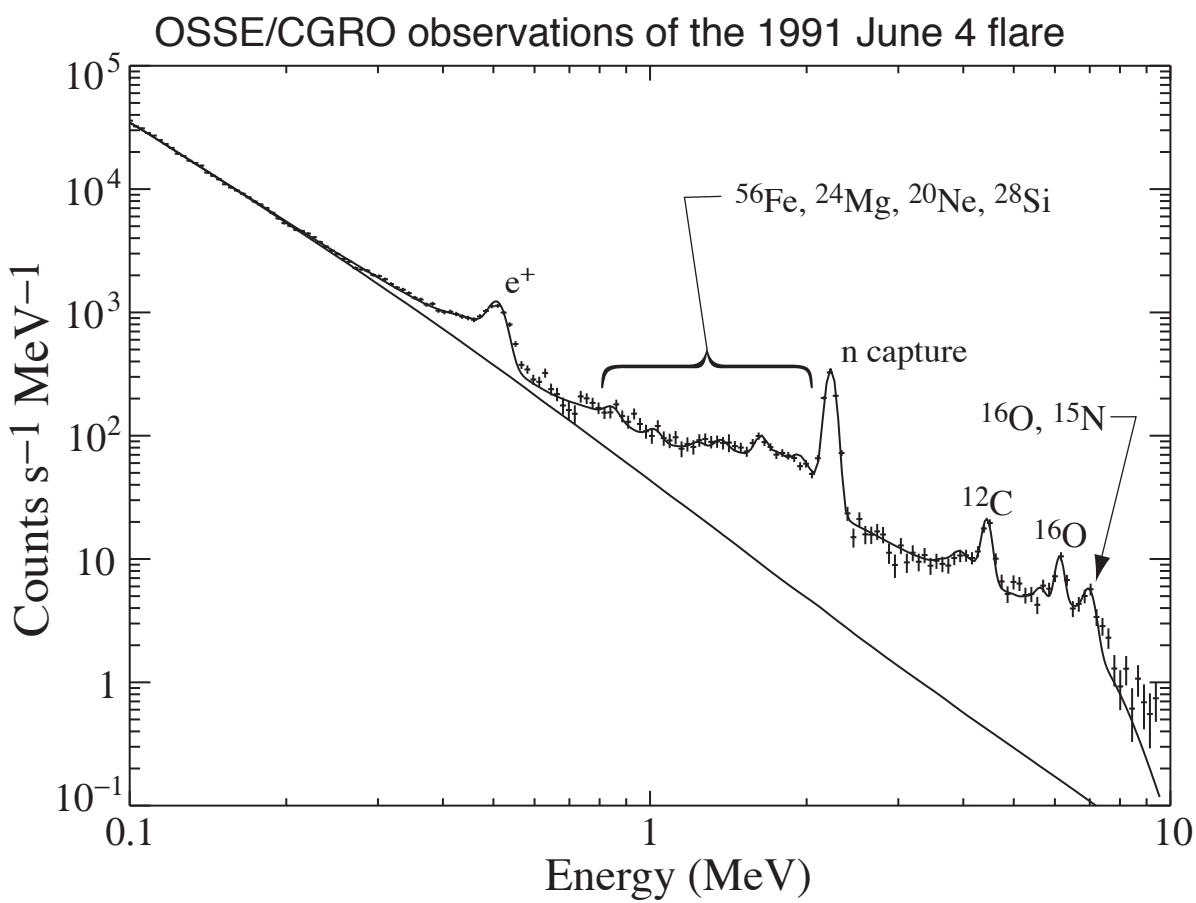

Data Samples
Neutron Data

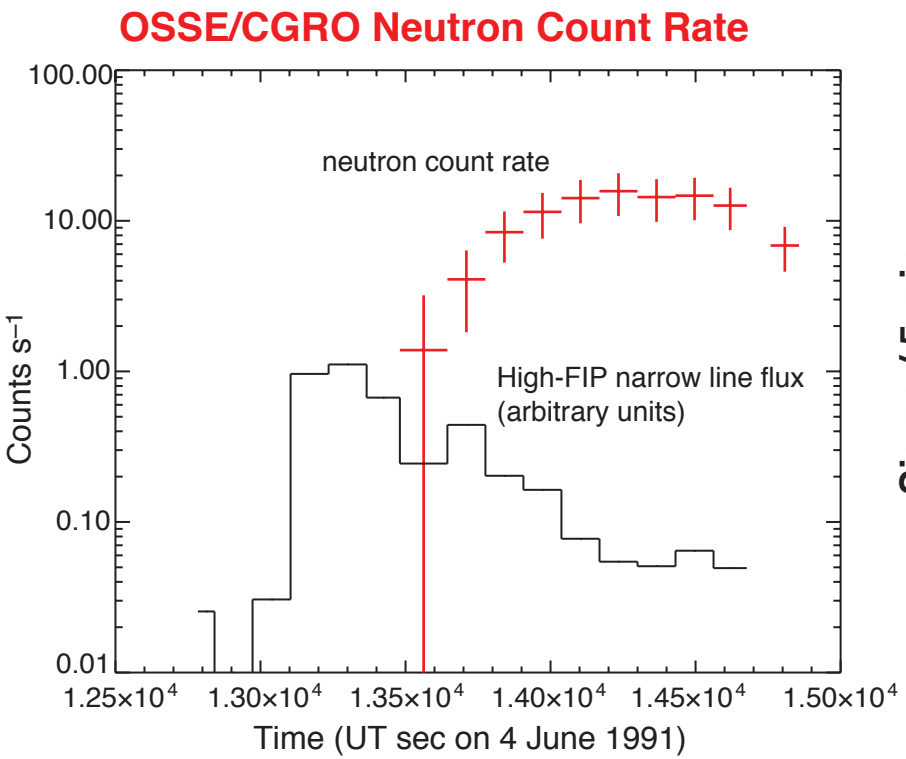

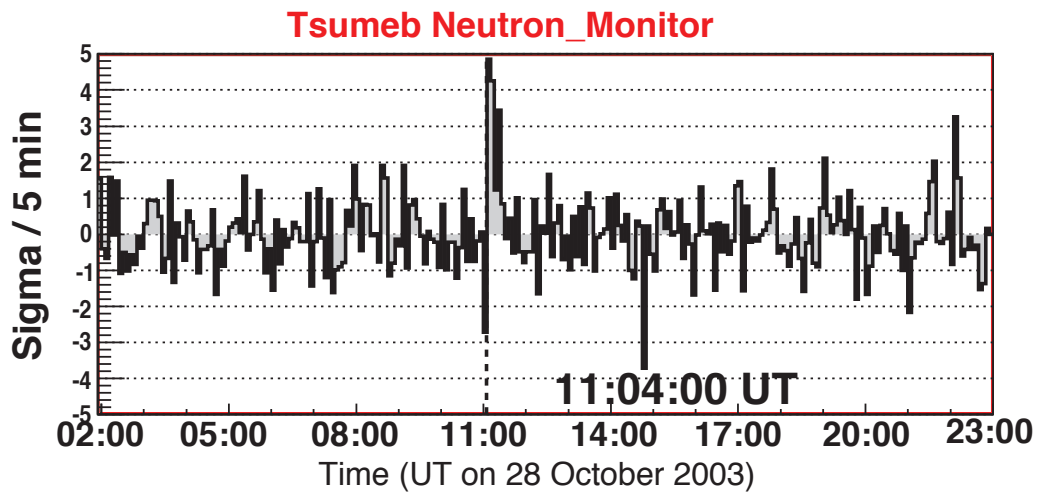

Data Samples
Background Spectrum

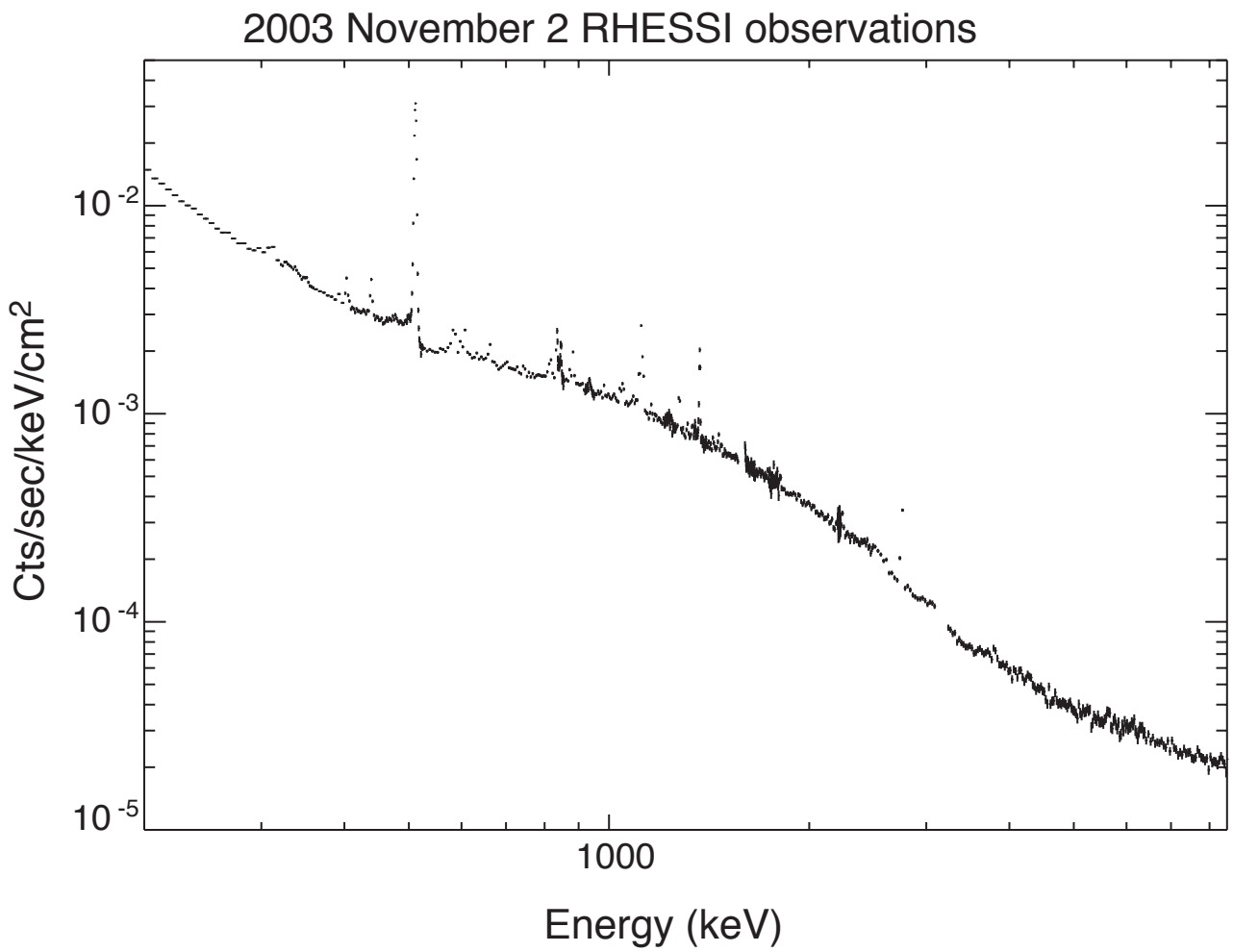

Data Samples
Flare + Background Spectra

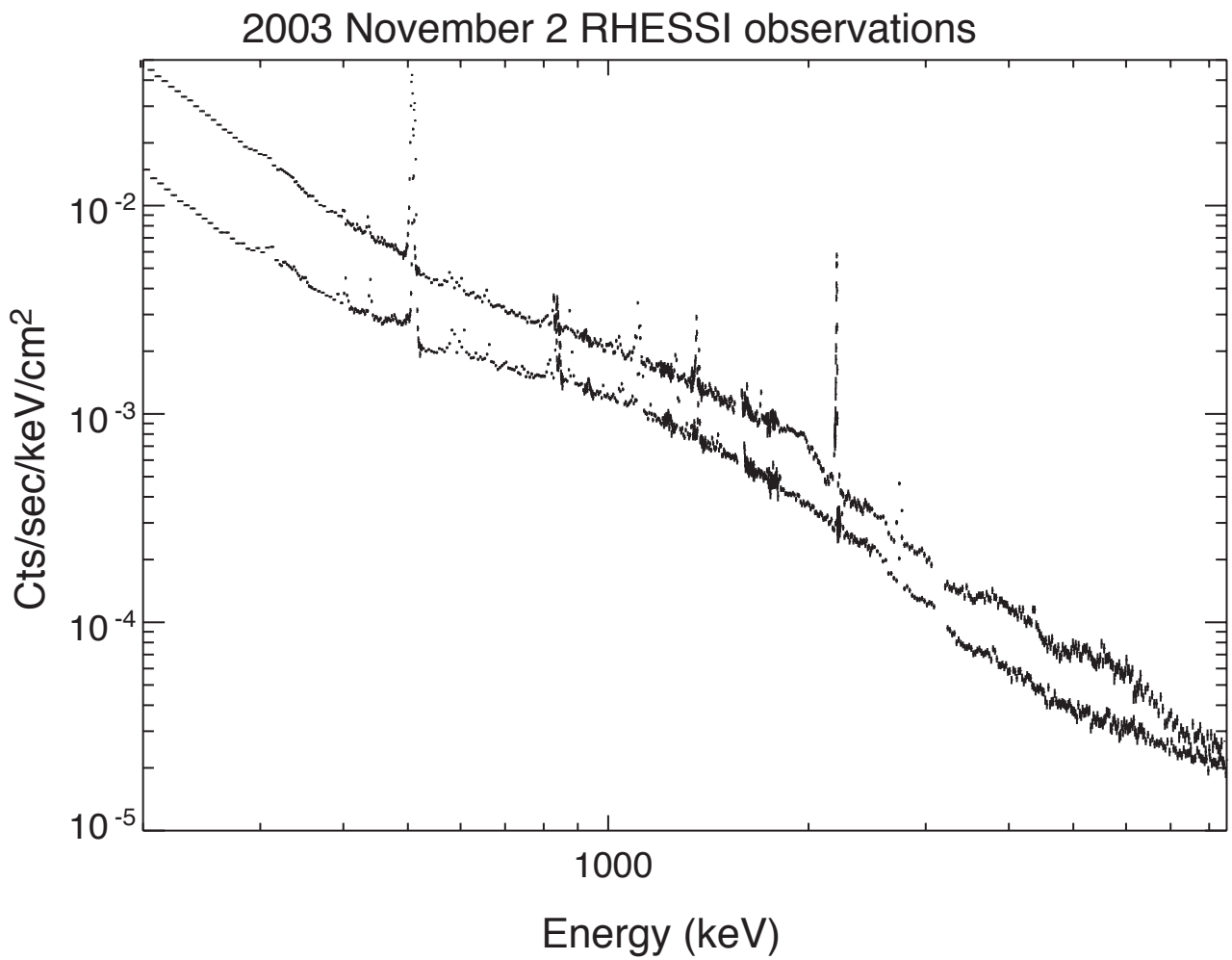

Data Samples
Difference Spectrum

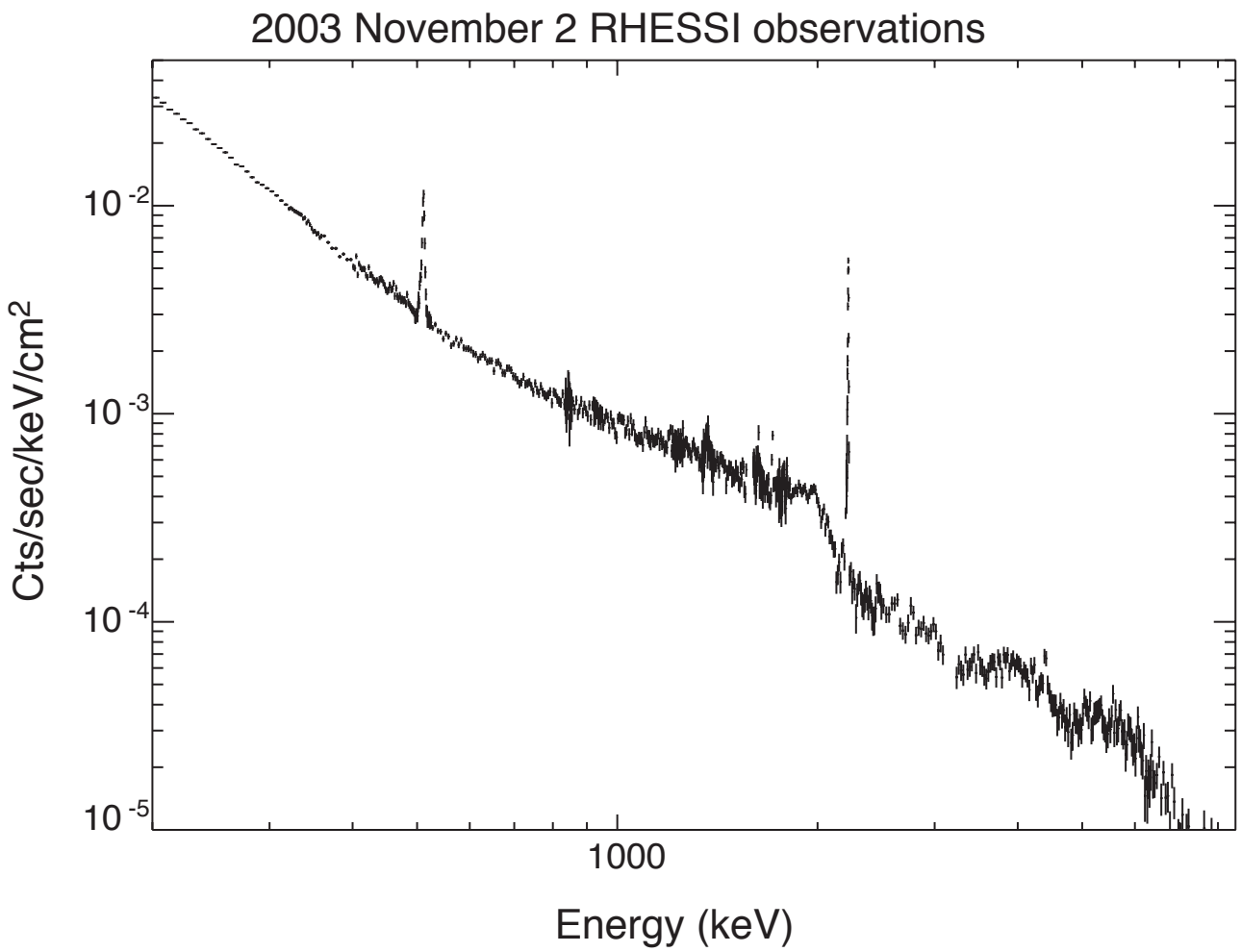

Data Samples
Positron Annihilation Line

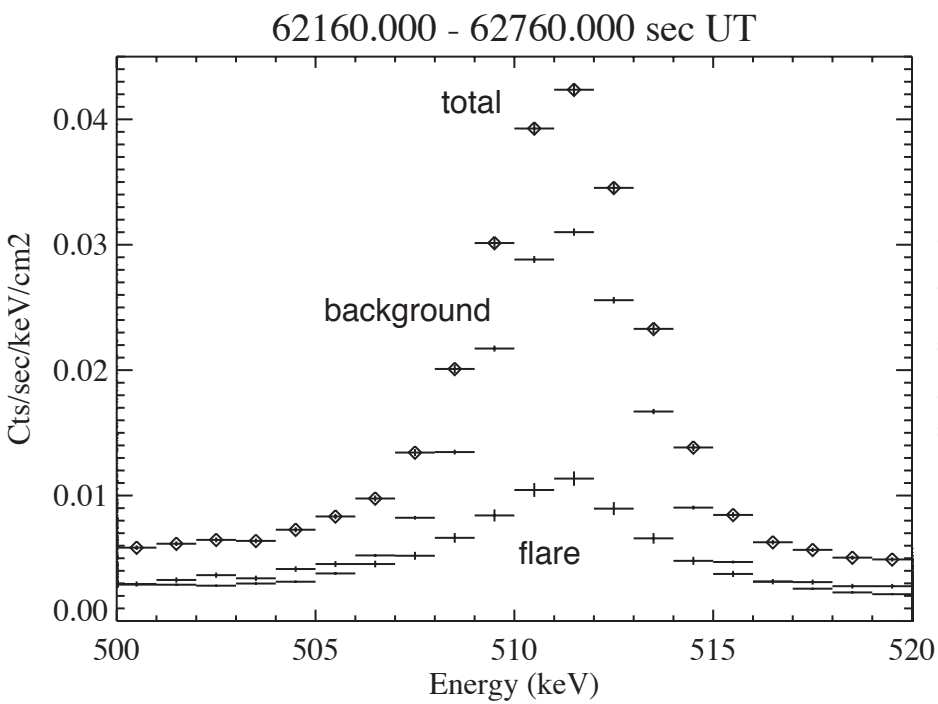

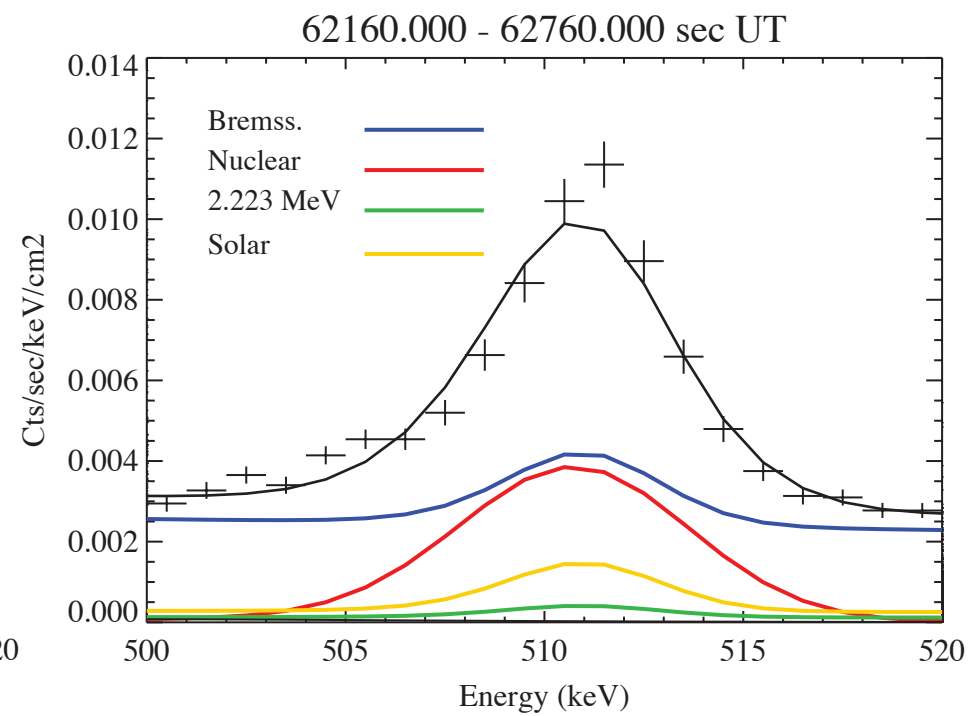

High-Energy Solar Flare Observable Quantities

Deexcitation lines

flux time history
total fluence
line profile (shape & shift)

Escaping neutrons

flux time history at detector (arriving time-dependent KE spectrum)
total fluence

Neutron-capture line

flux time history
total fluence

Positron annihilation line

flux time history
total fluence
line profile (shape & Ps continuum)

Pion-decay emission

flux time history
total fluence
time-dependent spectrum

Analysis of High-Energy Observable Emission

The traditional physics approach:

Develop a model for the flare process that can explain the observations with as few physically-based parameters as possible

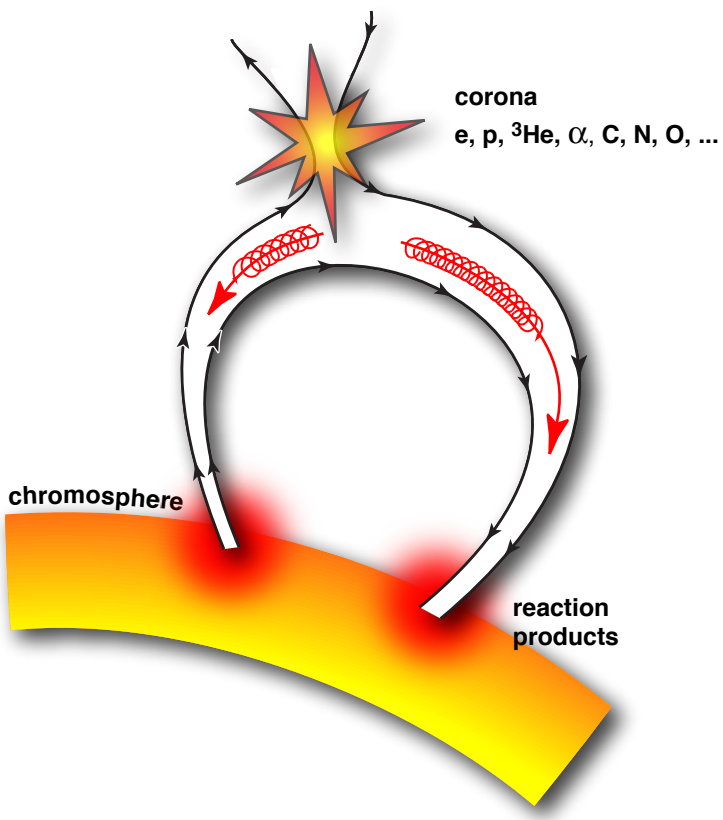

Transport and interaction model described by a set of parameters relating to conditions at the Sun,

$f(p_1, p_2, p_3, \ldots, p_n)$

↓

Predicted observable quantities

↓

Compare with measured observable quantities

↓

Modify parameters $p_1, p_2, p_3, \ldots, p_n$

Magnetic Loop Model

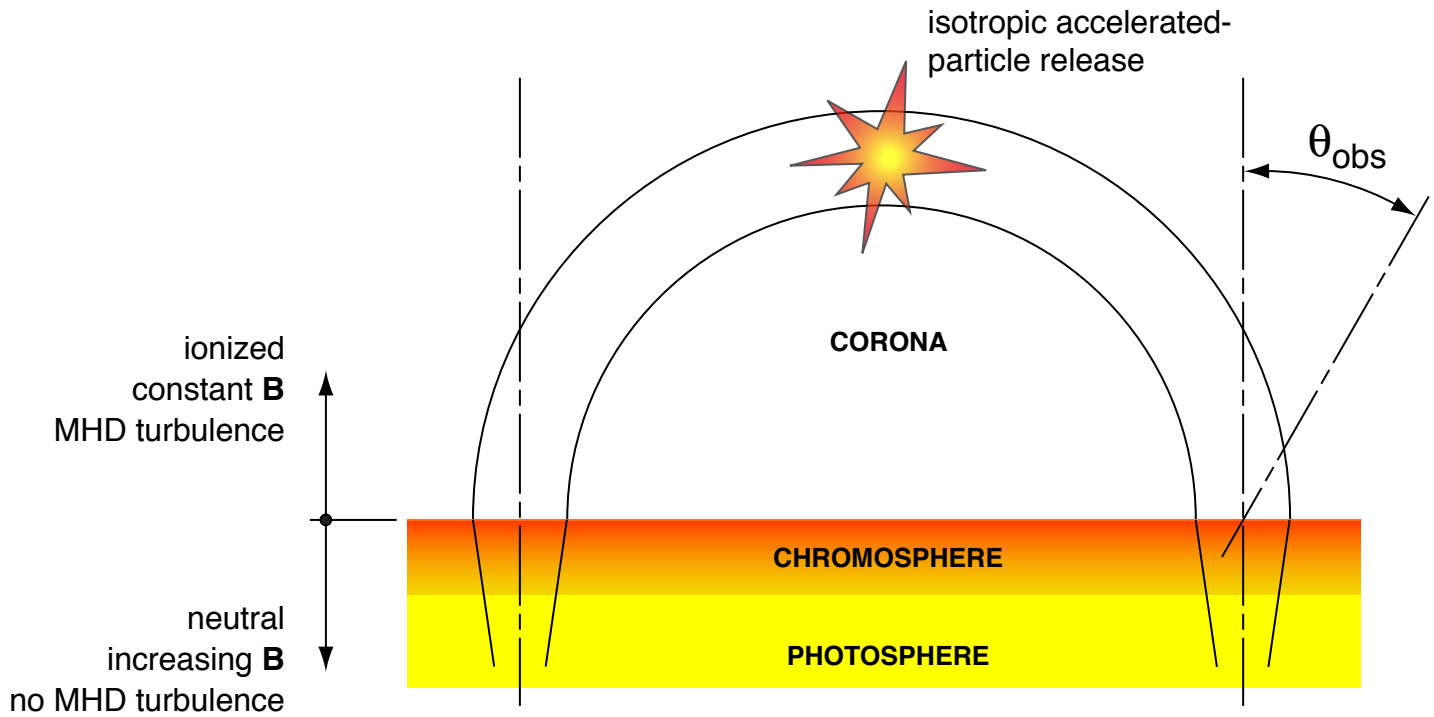

- Scattering due to MHD turbulence replenishes loss cone: $\lambda = \frac{\Lambda}{L_c}$ (mean free path) (loop half length)
- Mirroring due to magnetic field convergence: $B(h) \propto P(h)^{\delta}$
- Atmospheric model, n(h), T(h)
- Accelerated-particle spectral index, abundances
- ambient abundances
- **B** perpendicular to solar surface at footpoints

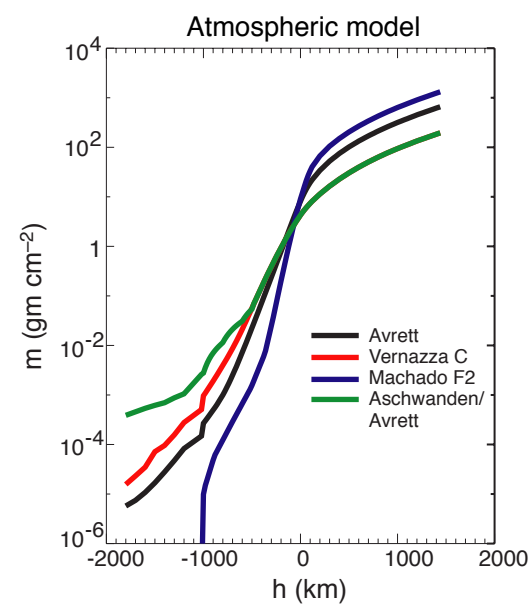

Magnetic Loop Model (cont.)
Parameter Summary

acceleration parameters	acceleration release time history	$a_{ion}(t)$
	spectrum (power-law spectral index)	s
	accelerated ion composition	N_i
physical parameters	loop length	L
	level of pitch-angle scattering	λ
	magnetic convergence	δ
	ambient composition	n_i
	atmospheric model	$n(h)$
	flare heliocentric angle	θ_{obs}

Consequences of the Transport Model

consider

three aspects

of the interacting accelerated ions that are affected by transport and that will subsequently affect the observable quantities

1. the time history of the interactions due to transport
2. the depth distribution of the interactions
3. the angular distribution of the interacting ions

Consequences of the Transport Model

The number of possible parameter combinations is very large

vary one of the parameters while holding the other parameters fixed at standard values:

$\lambda = 300$
$\delta = 0.2$
L = 11,500 km
s = 4
Avrett (1981) sunspot region atmosphere
accelerated $\alpha/p = 0.5$

We will use production of the ^{12}C 4.438 MeV line as an example for discussion.
Other nuclear reactions will behave similarly.

Intertacting Ion Angular Distribution

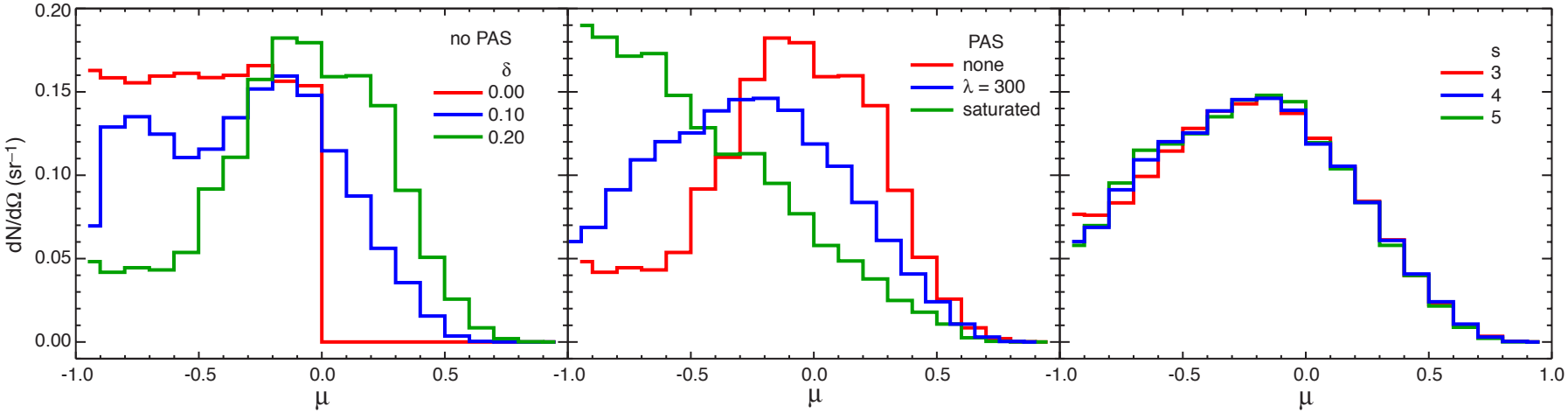

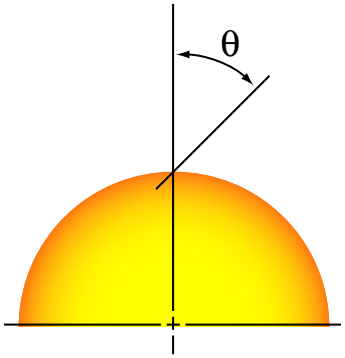

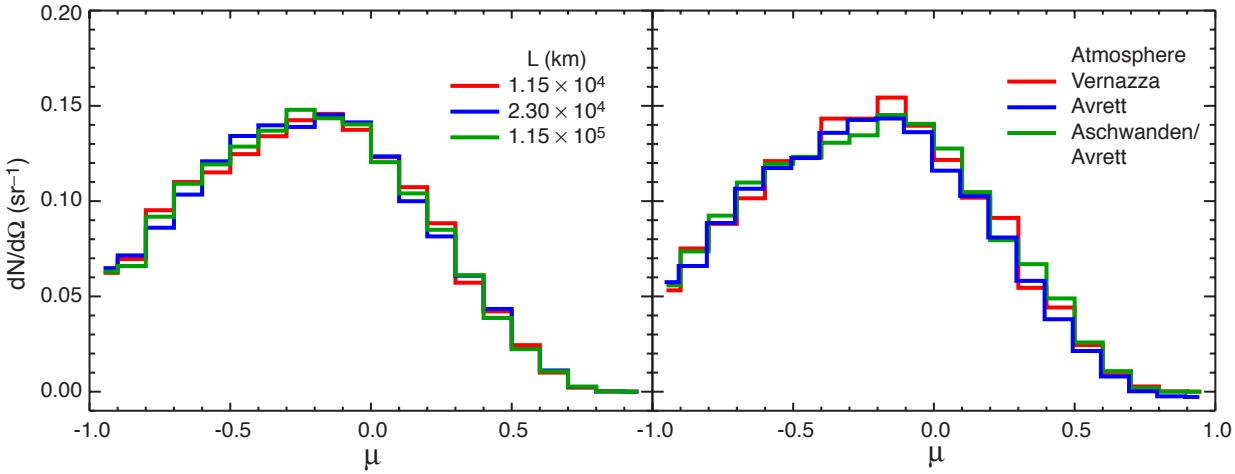

$\mu = \cos(\theta)$

$\mu > 0 \Longrightarrow$ upward

$\mu < 0 \Longrightarrow$ downward

Depth of Interactions

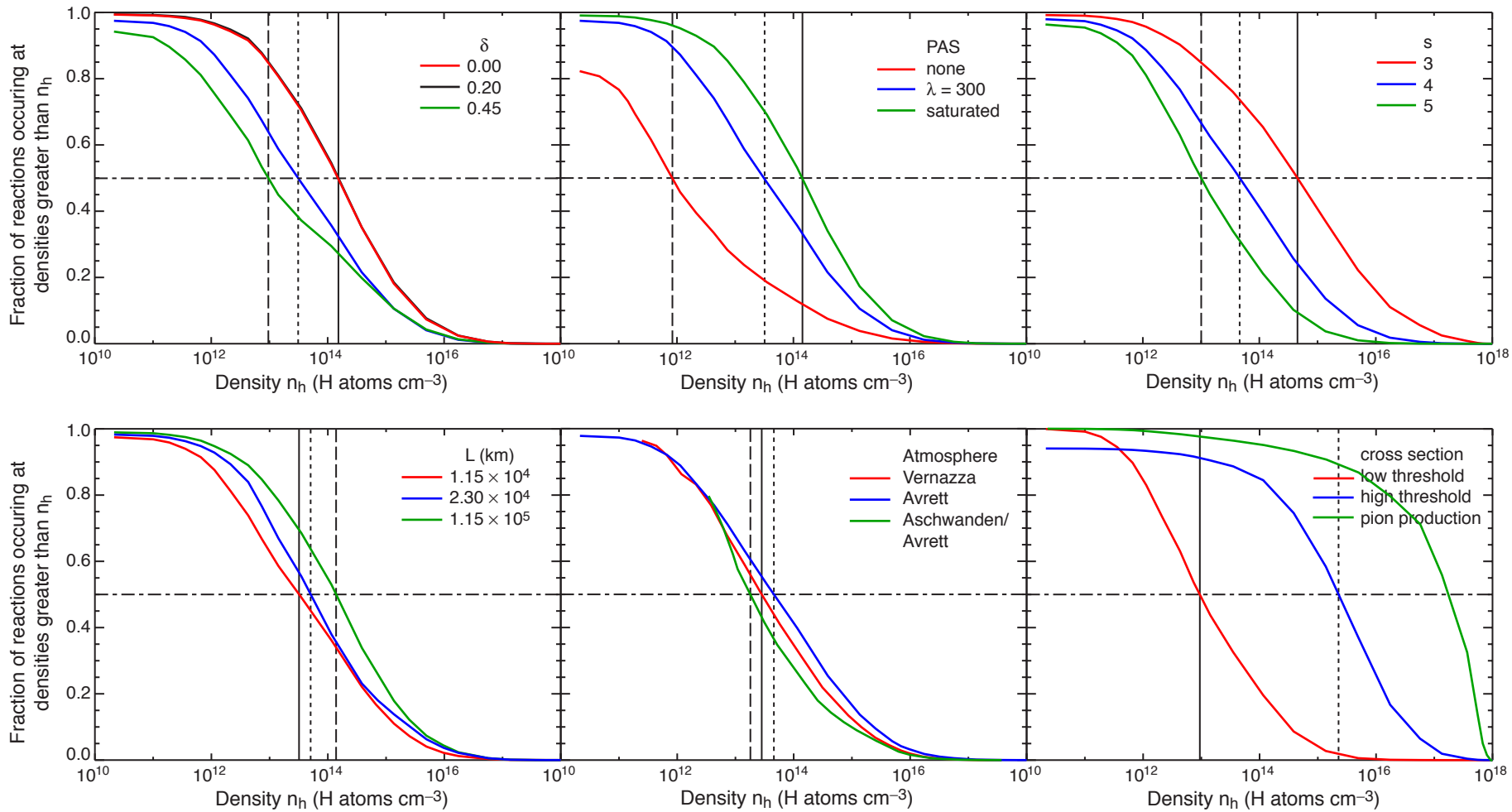

Interaction Time History (instantaneous injection)

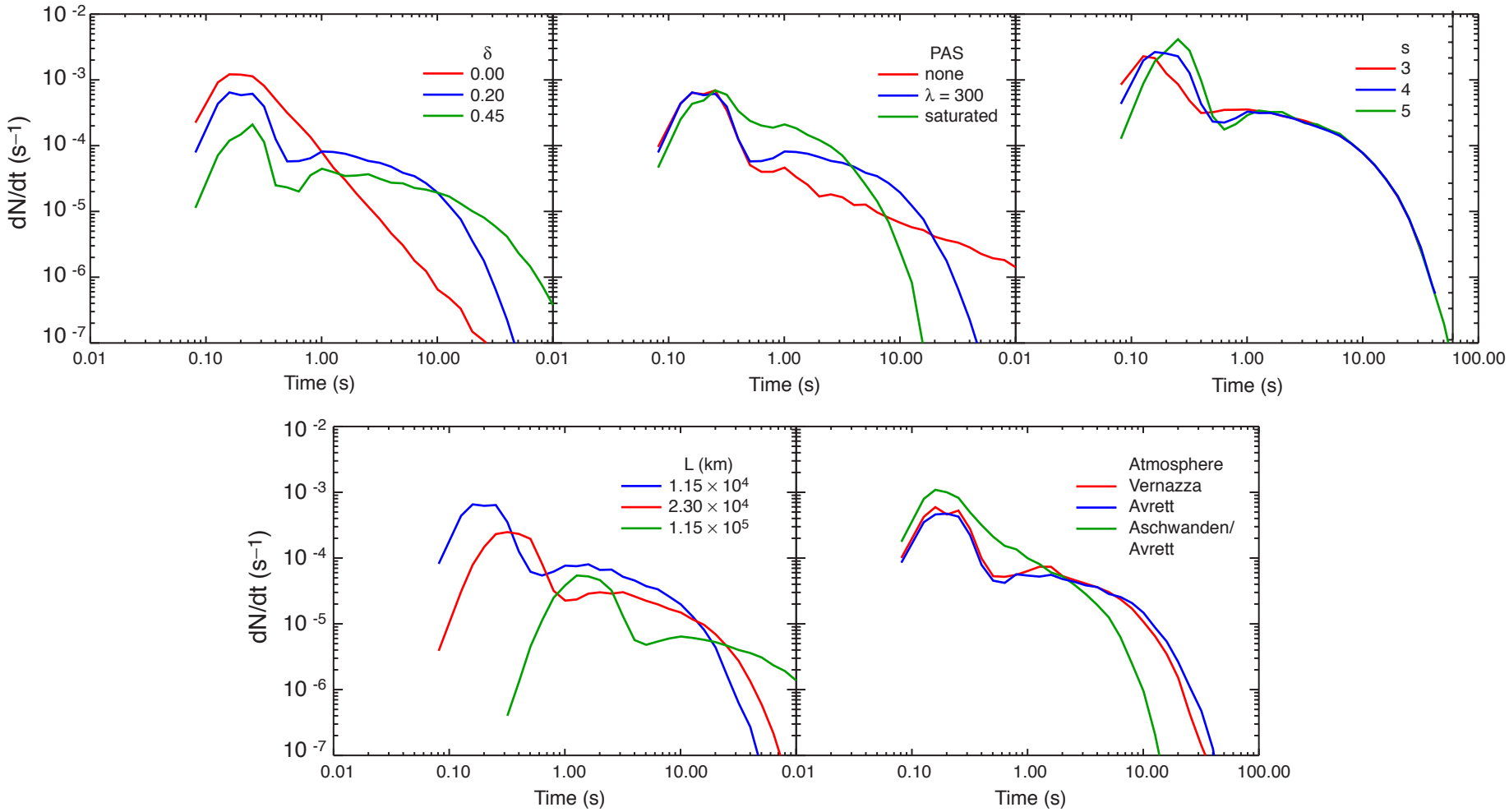

Summary of the Dependence of Observable Quantities on the Parameters

Observable	Acceleration Parameter	Physical Parameter
narrow deexcitation line fluences & ratios	α/p, s	ambient abundances
narrow deexcitation line shift and shape	α/p, s	δ, λ, θ_{obs}, $n(h)$
narrow deexcitation line time history	$a_{\mathrm{ion}}(t)$	δ, λ, L_c, $n(h)$
neutron fluence at Earth	α/p, s	δ, λ, θ_{obs}, $n(h)$
neutron arrival time history at Earth	$a_{\mathrm{ion}}(t)$, α/p, s	δ, λ, θ_{obs}, L_c, $n(h)$
neutron-capture line fluence	α/p, s	δ, λ, θ_{obs}, $n(h)$, ambient $^3\mathrm{He}/\mathrm{H}$
neutron-capture line time history	$a_{\mathrm{ion}}(t)$, α/p, s	δ, λ, θ_{obs}, L_c, $n(h)$, ambient $^3\mathrm{He}/\mathrm{H}$
511 keV line shape and continuum	α/p,$^3\mathrm{He}/\,^4\mathrm{He}$, s	δ, λ, θ_{obs}, $n(h)$, $T(h)$, $X(h)$
511 keV line time history	$a_{\mathrm{ion}}(t)$, α/p, s acc. abundances	δ, λ, θ_{obs}, L_c, $n(h)$, $X(h)$
511 keV line fluence	α/p, s,$^3\mathrm{He}/\,^4\mathrm{He}$ acc. abundances	δ, λ, θ_{obs}, $n(h)$, $T(h)$, $X(h)$

Effect of Model Parameters on the Observable Quantities

Deexcitation LineYields

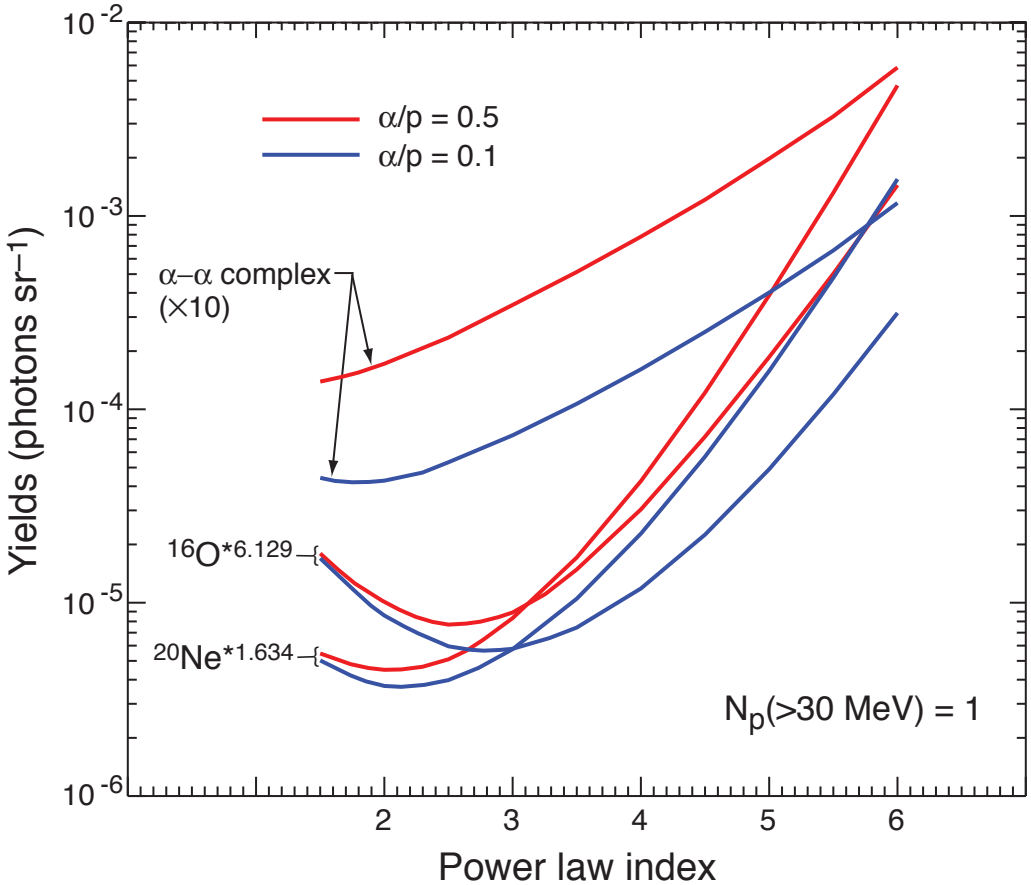

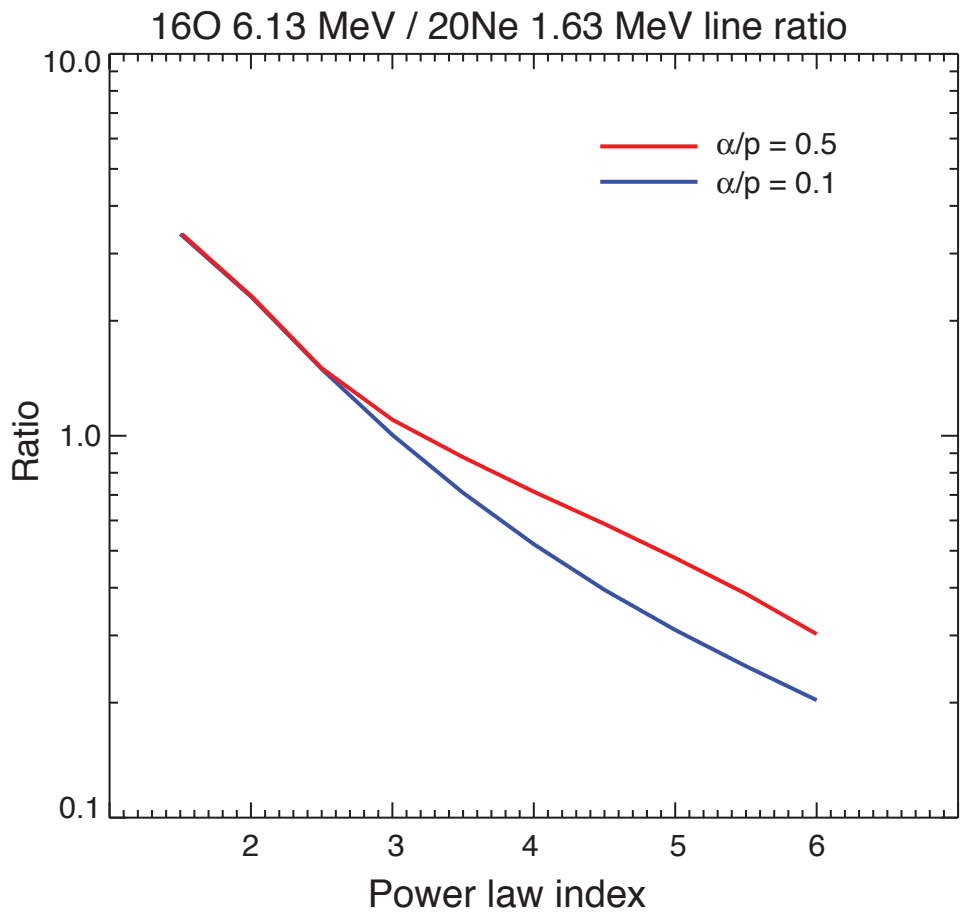

$\alpha + {}^{4}He \longrightarrow {}^{7}Be^{*0.429} + n$

$\alpha + {}^{4}He \longrightarrow {}^{7}Li^{*0.478} + p$

Effect of Model Parameters on the Observable Quantities

Deexcitation Line Shape

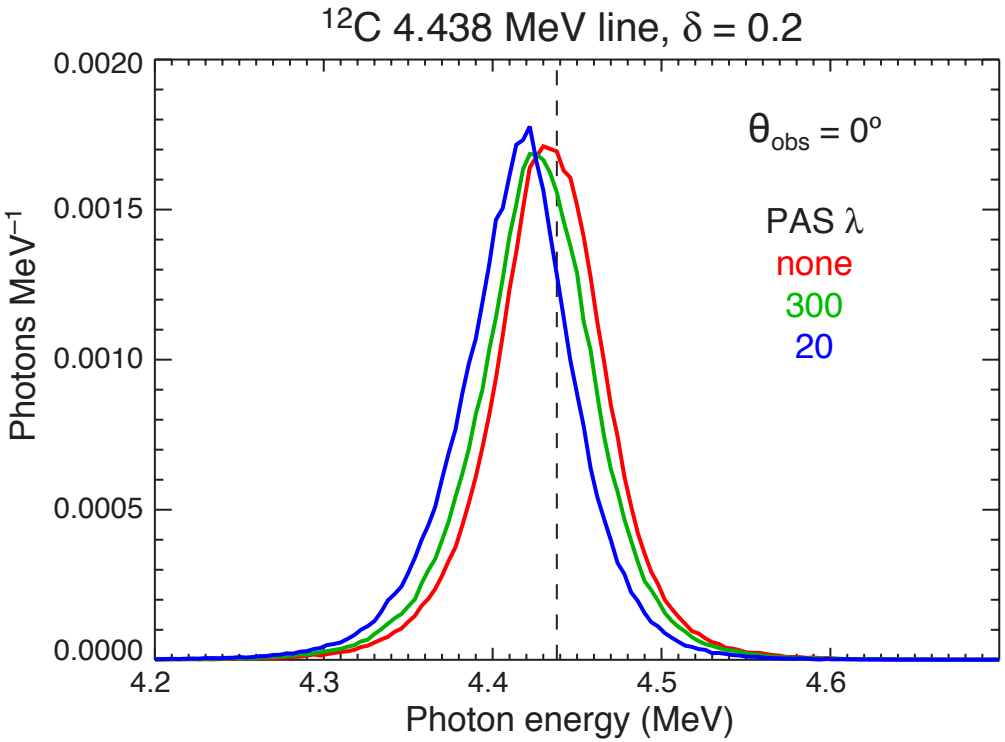

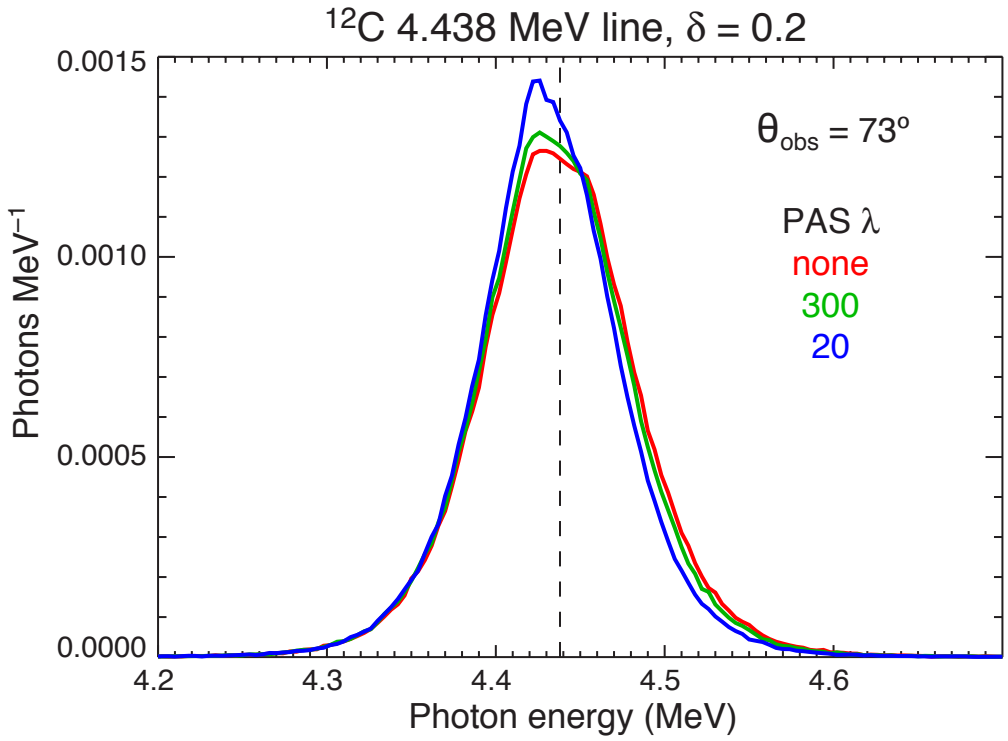

Effect of Model Parameters on the Observable Quantities

Neutron & Neutron-Capture Line Yields

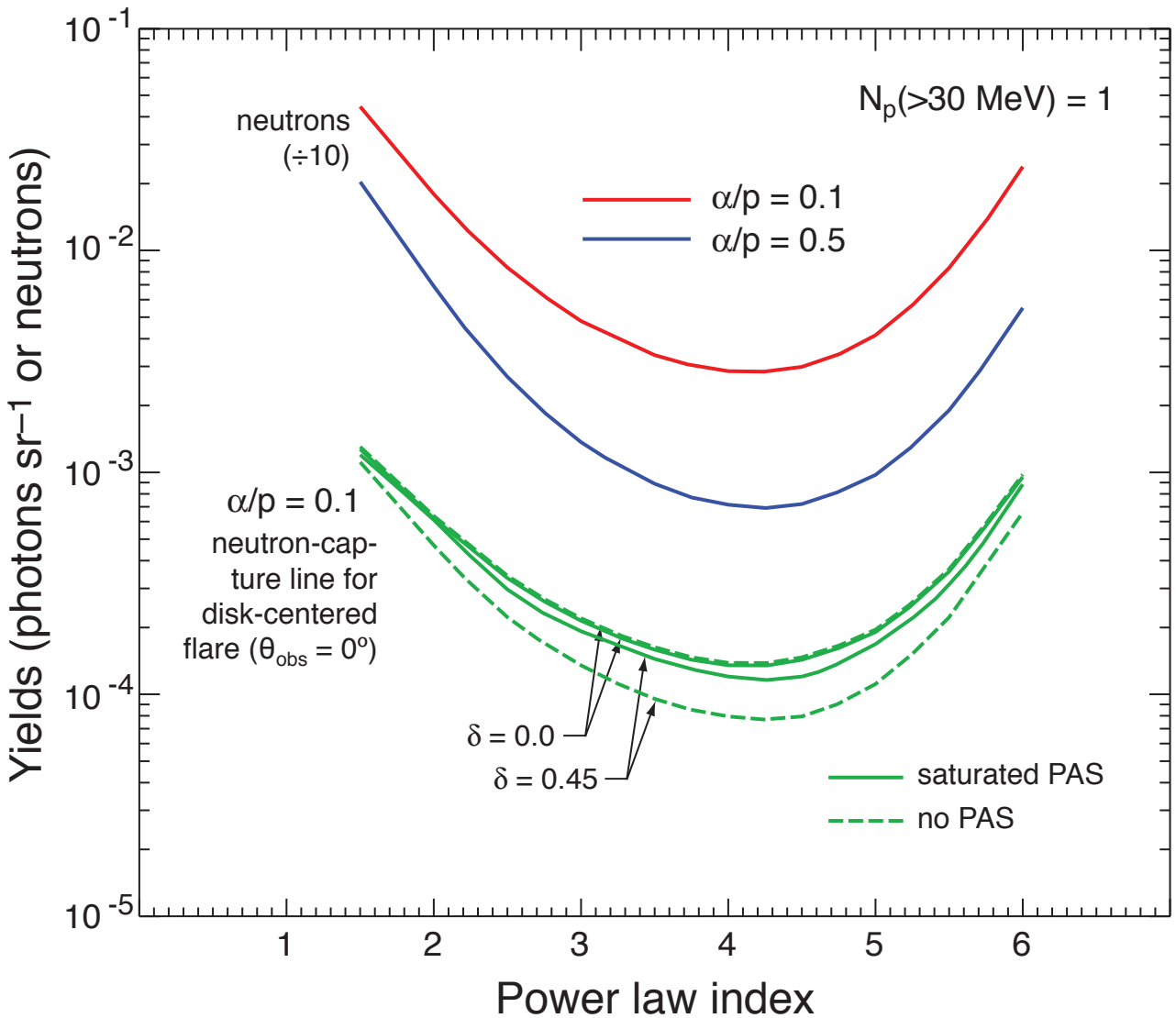

Effect of Model Parameters on the Observable Quantities

Escaping Neutron Spectra

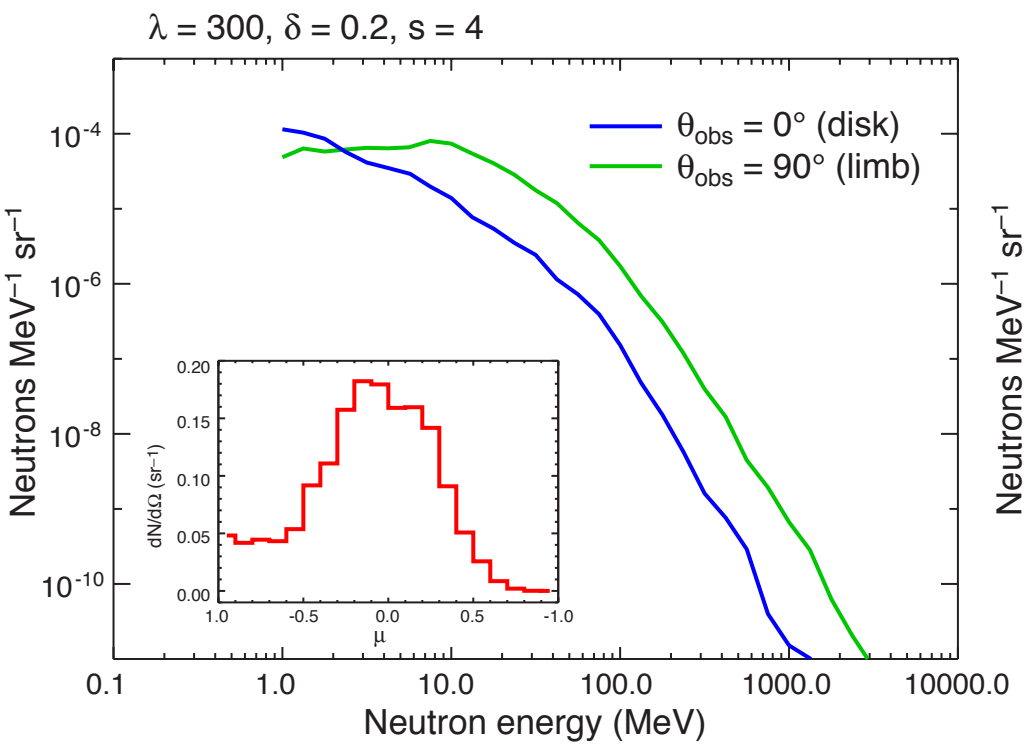

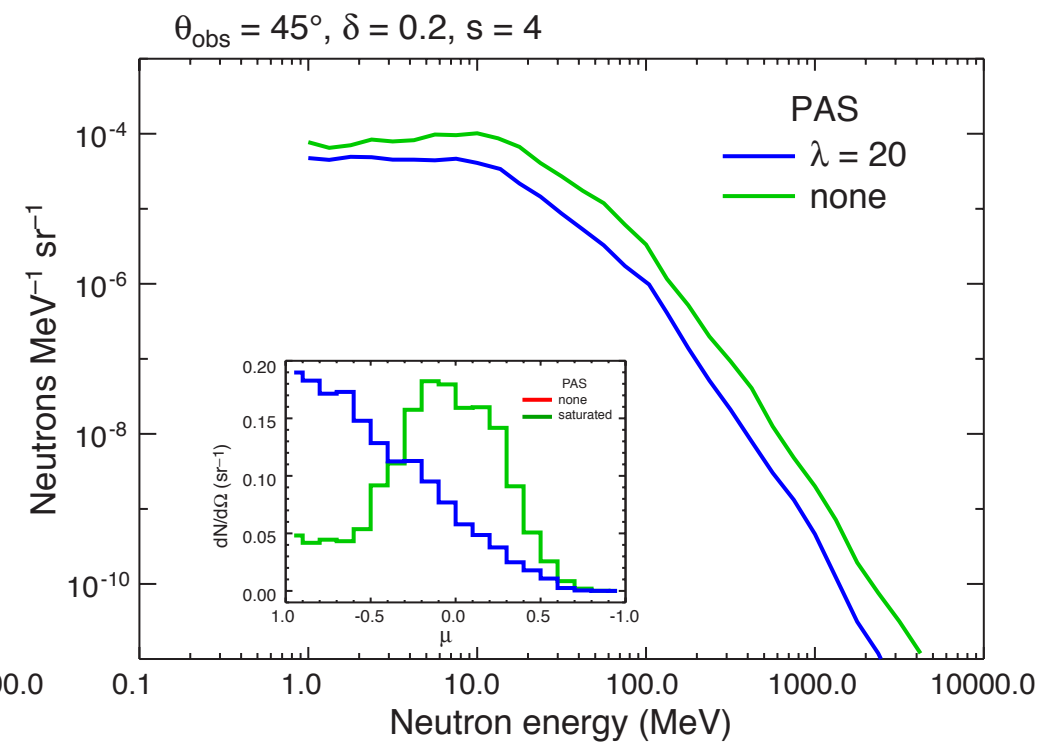

Neutron-capture Line Time History (instantaneous injection)

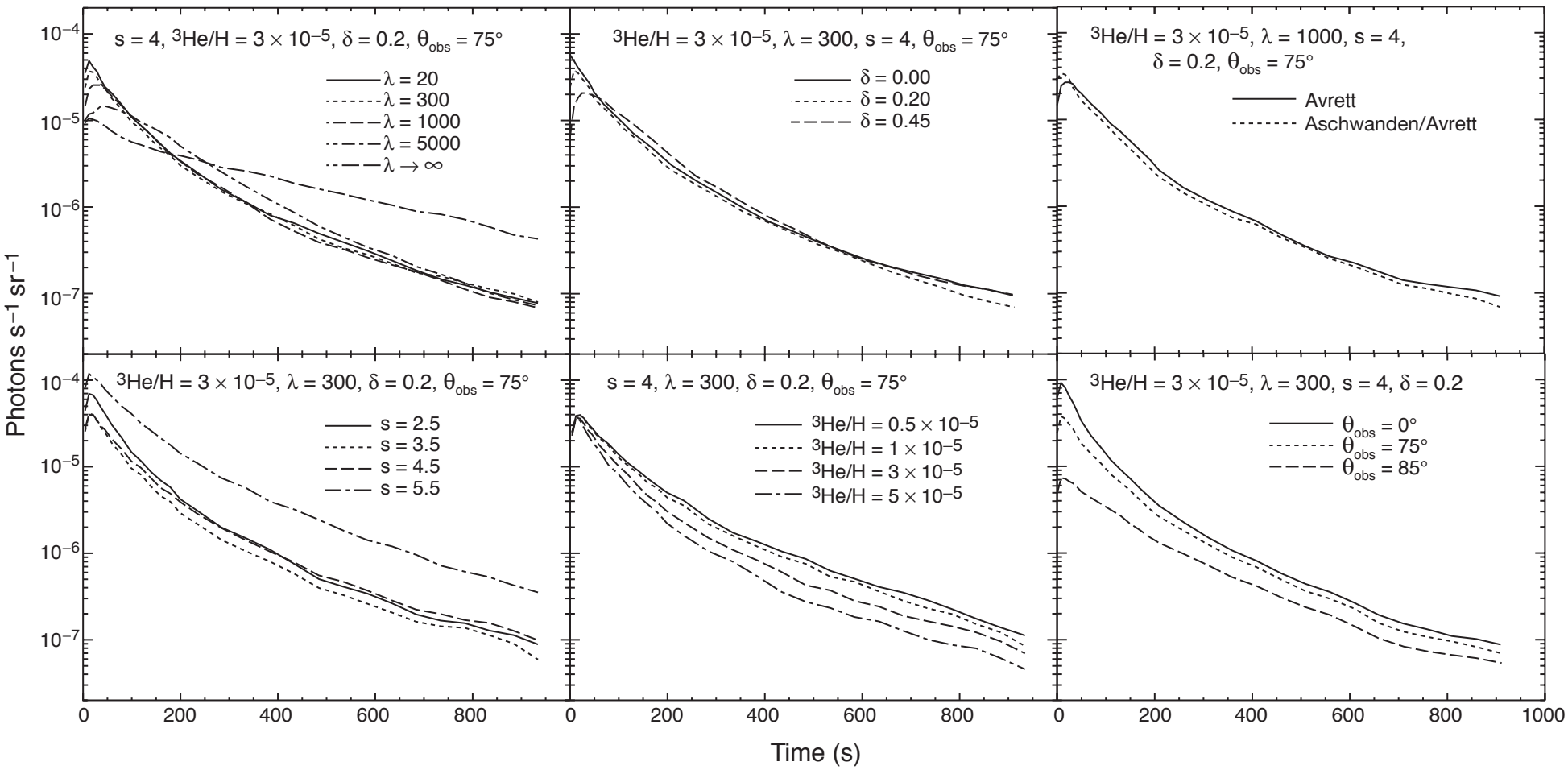

Effect of Model Parameters on the Observable Quantities

Annihilation Line Shapes

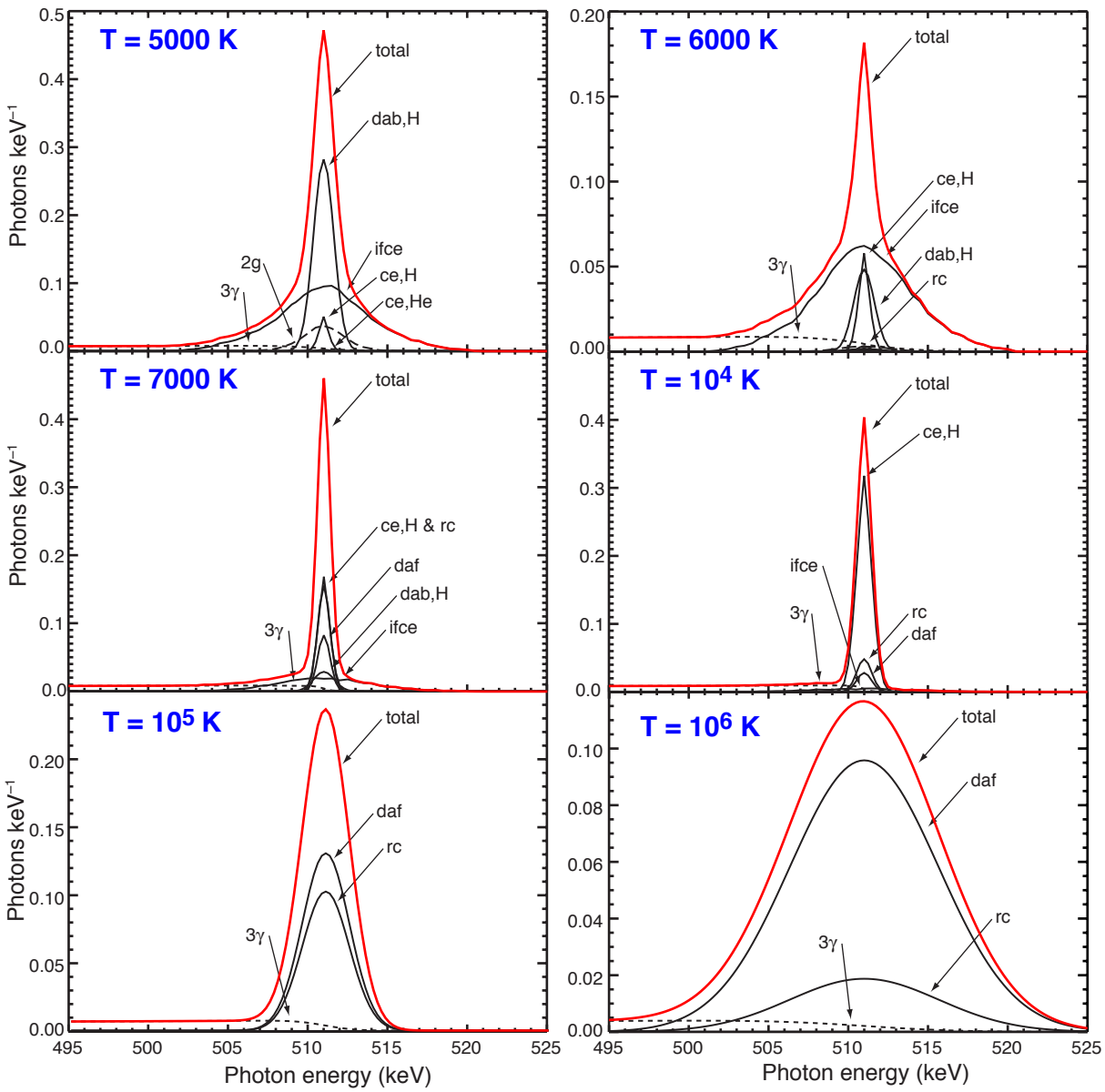

Effect of Model Parameters on the Observable Quantities

Annihilation Line Depth Distribution

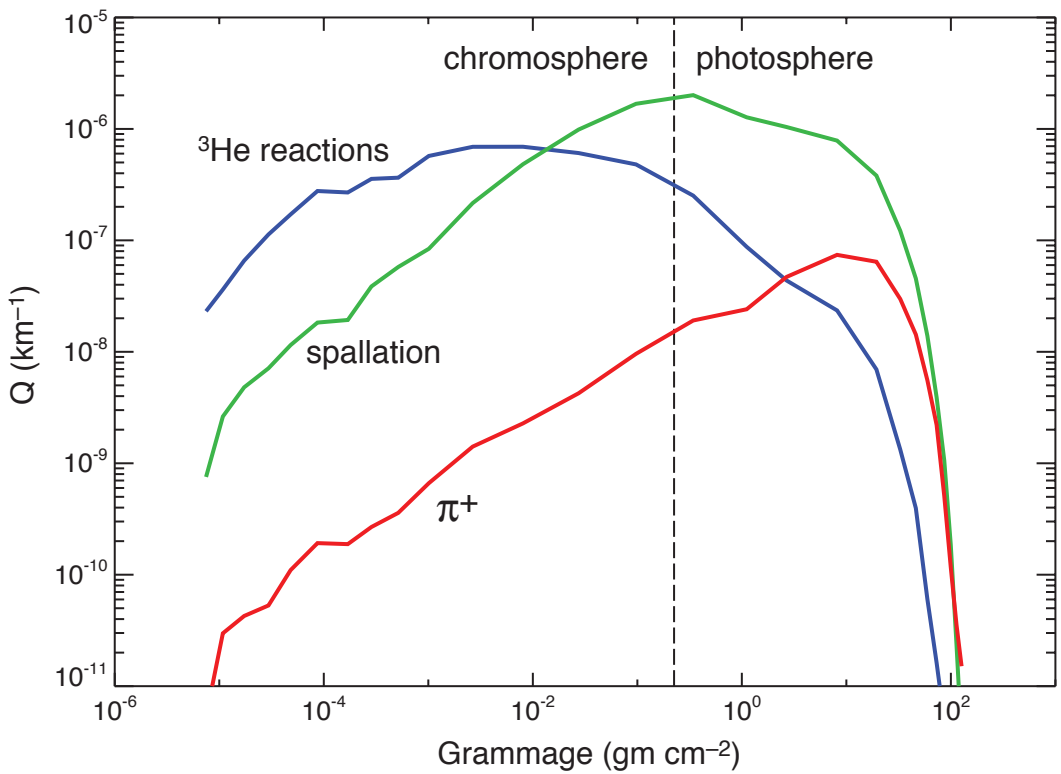

	θ_{obs}	transmission
low thresh (^{3}He radioactive)	0	0.95
	30	0.95
	60	0.93
high threshold (spallation radioactive)	0	0.61
	30	0.59
	60	0.52
pion threshold	0	0.15
	30	0.14
	60	0.11

Data Analysis Approach

Problem:

While the number of observable quantities is potentially large, they depend in complex and over-lapping ways on a large number of model parameters.

Solutions:

1. **For flares that offer a sufficiently-wide range of measured observables, attempt to address all dependences through a systematic analysis approach, starting with observables with the simplest parameter dependences and progressing to observables with more complex dependences.**

2. **For less well-measured flares, determine only a subset of parameters, ignoring the other parameters by fixing them at reasonable values, allowing constraints to be set on the rest. Estimate resulting systematic uncertainties.**

Data Analysis of the 1991 June 4 Flare

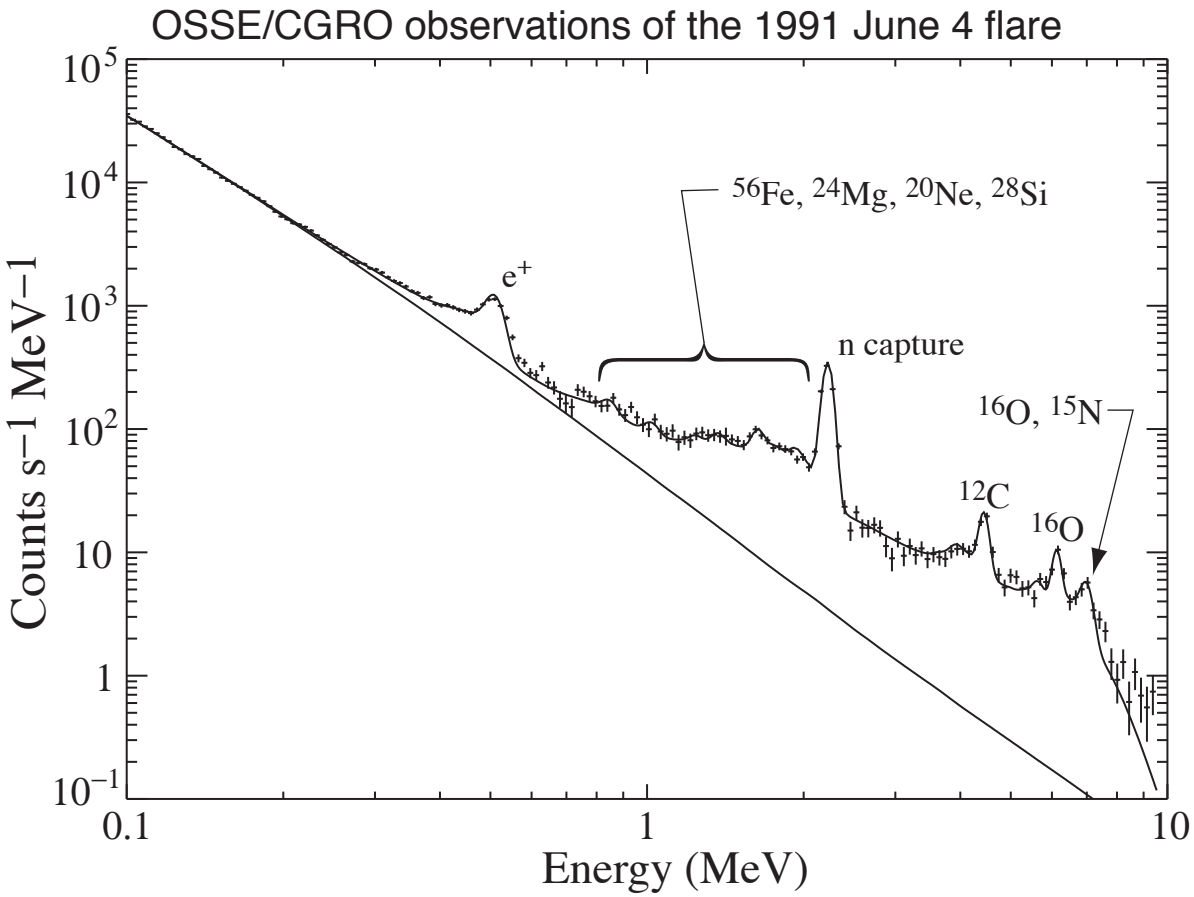

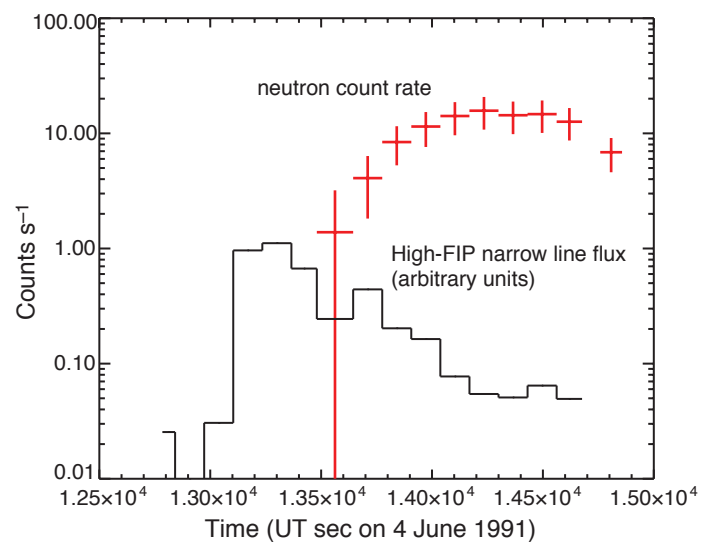

Data Analysis of the 1991 June 4 Flare
Loop Size

White light images of footpoints at 3:40:34 UT

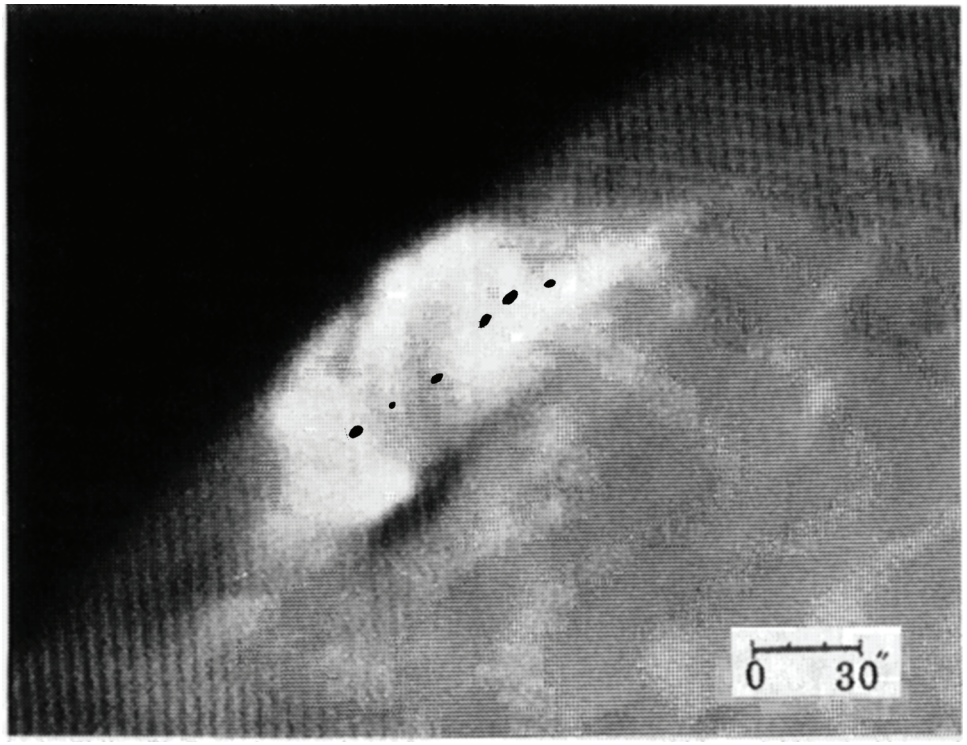

Sakurai et al. 1991

11,500 km < L < 65,000 km

Data Analysis of the 1991 June 4 Flare
α/proton Ratio and Spectral Index

use the α–α complex, ^{12}C 4.44 MeV, ^{16}O 6.13 MeV, and ^{20}Ne 1.63 MeV line ratios

$$\frac{\phi_{6.13}}{\phi_{1.63}} = 0.66 \pm 0.07$$

$$\frac{\phi_{\sim 450}}{\phi_{4.44}} = 0.66 \pm 0.04$$

s = 3.9 ± 0.2

α/p > 0.4

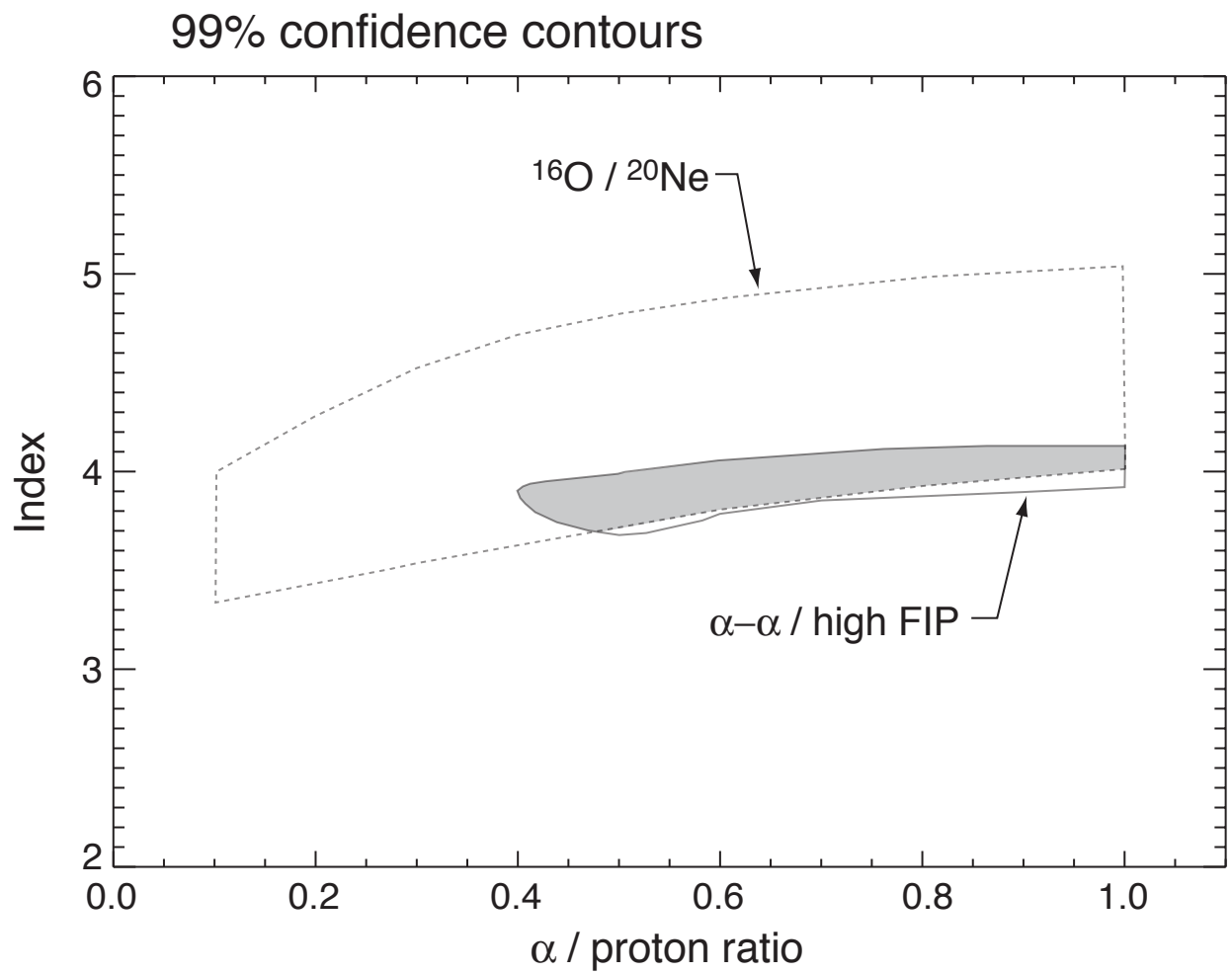

Data Analysis of the 1991 June 4 Flare
constraints on λ and δ

want to use the line centroid shift of the ^{12}C 4.44 MeV line

but the flare occurred at $\theta_{obs} = 74°$

$\varepsilon_0 = 4.442 \pm 0.005$ MeV

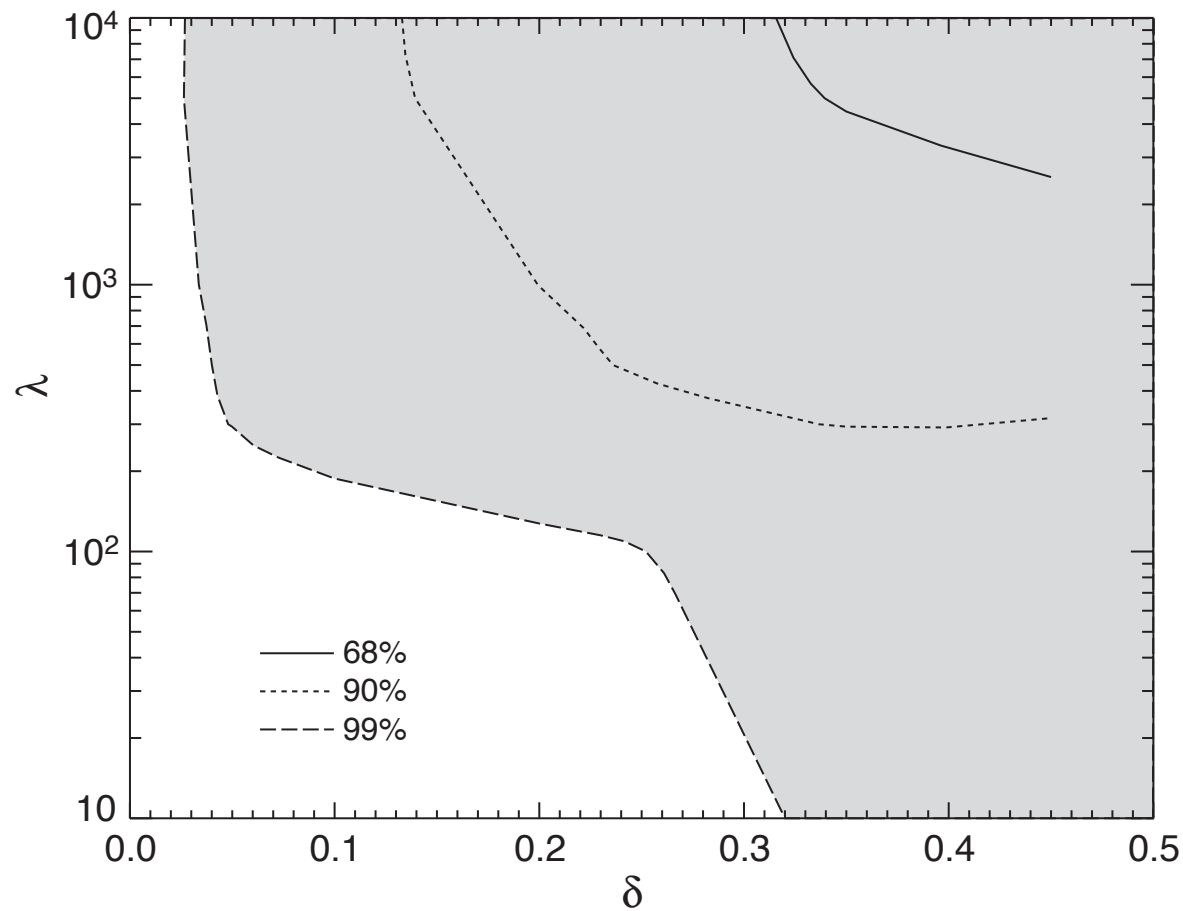

Data Analysis of the 1991 June 4 Flare
constraints on λ and δ

use the time history of the summed narrow deexcitation lines

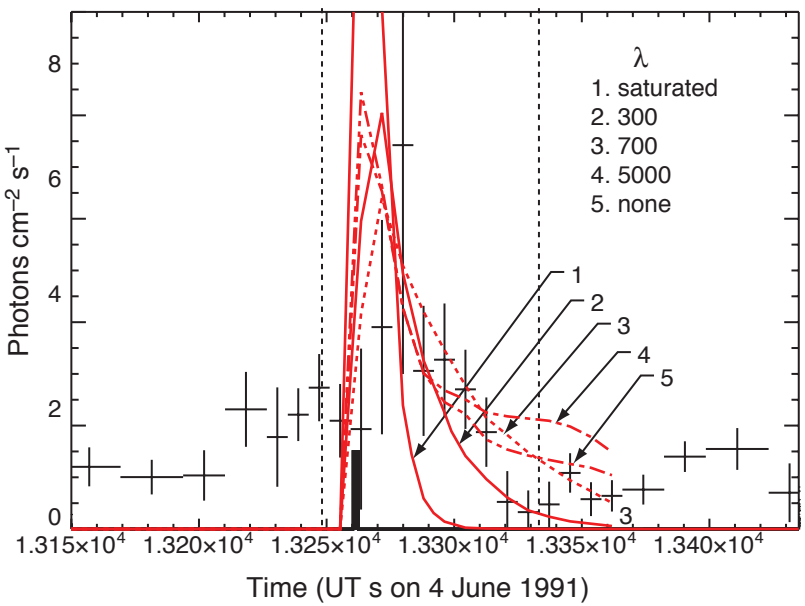

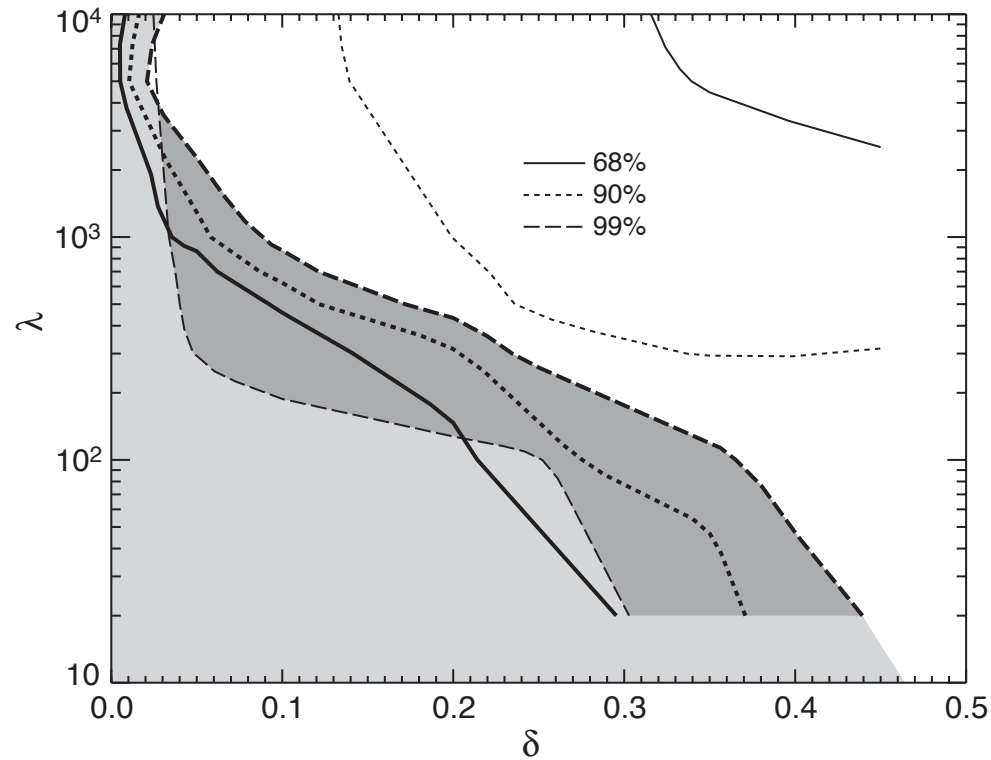

Data Analysis of the 1991 June 4 Flare
constraints on photospheric ^{3}He/H

data for the 2.223 MeV neutron-capture line remain
and the most important parameters have all been constrained
except for photospheric ^{3}He/H

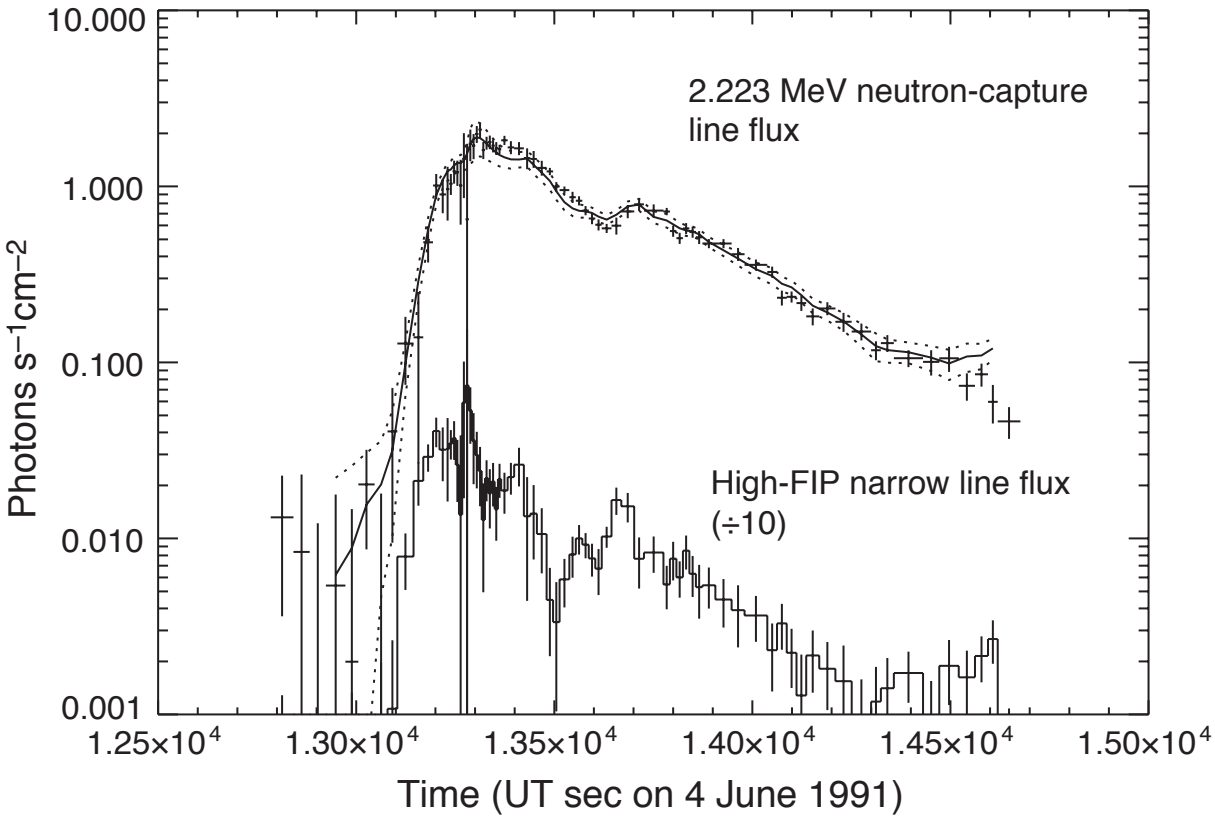

^{3}He/H < 4.5 × 10^{-5} (3-σ)

using recent measurements of ^{3}He/H in the solar wind and D/H and ^{3}He/^{4}He measurements at Jupiter, the bestestimate of photospheric ^{3}He/H is (3.7 ± 0.9) × 10^{-5}

Data Analysis of the 1991 June 4 Flare constraints on the high-energy behavior of the accelerated-particle energy spectrum

data for the escaping neutrons remain

and can be used to check for consistency

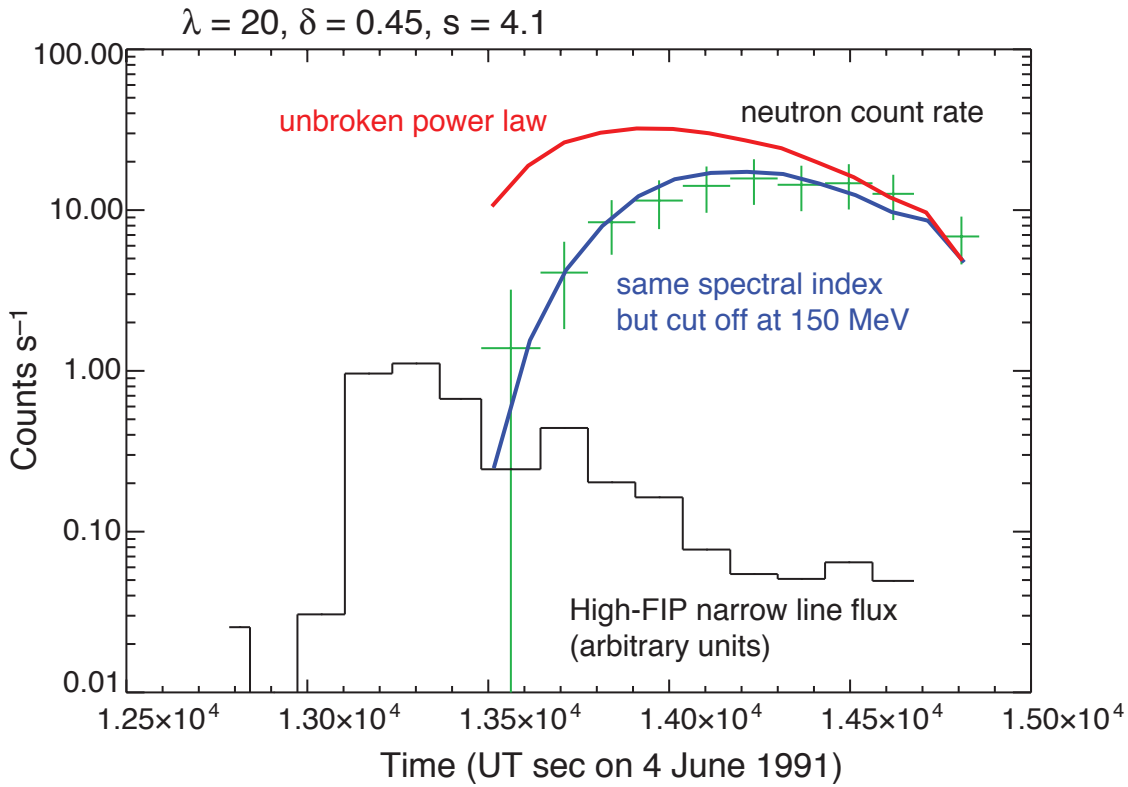

The count rate is overpredicted at early times implying too many high-energy neutrons.

So introduce a high-energy cut off to the accelerated-ion kinetic-ienergy spectrum to compensate.

150 MeV nucleon^{-1} works well.

Data Analysis of the 1991 June 4 Flare constraints on the high-energy behavior of the accelerated-particle energy spectrum

This does not modify earlier results since those emissions are produced by accelerated ions of energies less than 150 MeV nucleon^{-1}

Effective accelerated ion energies

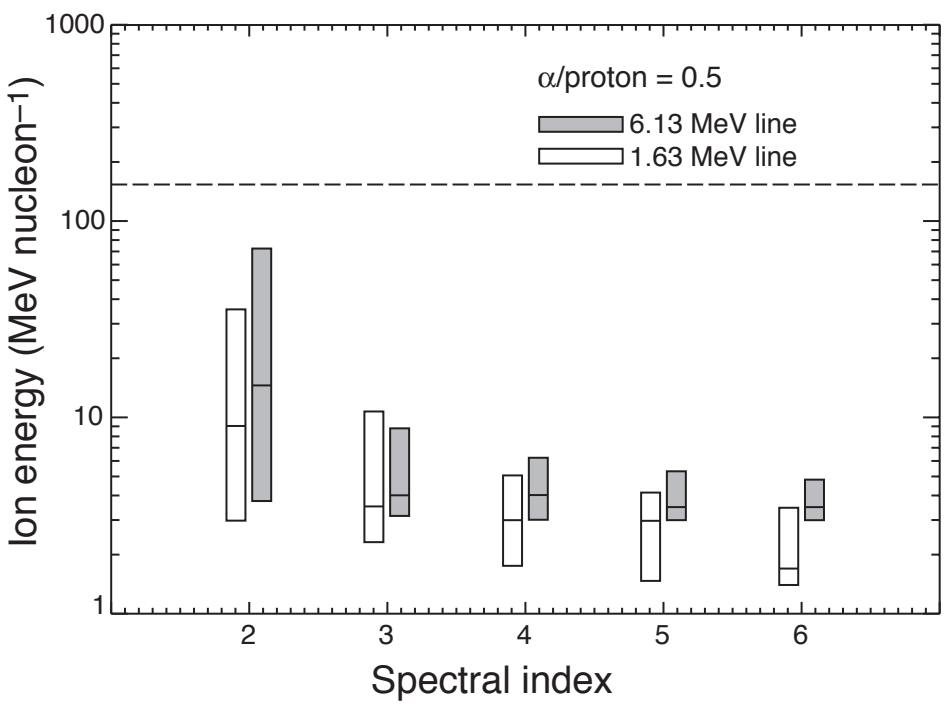

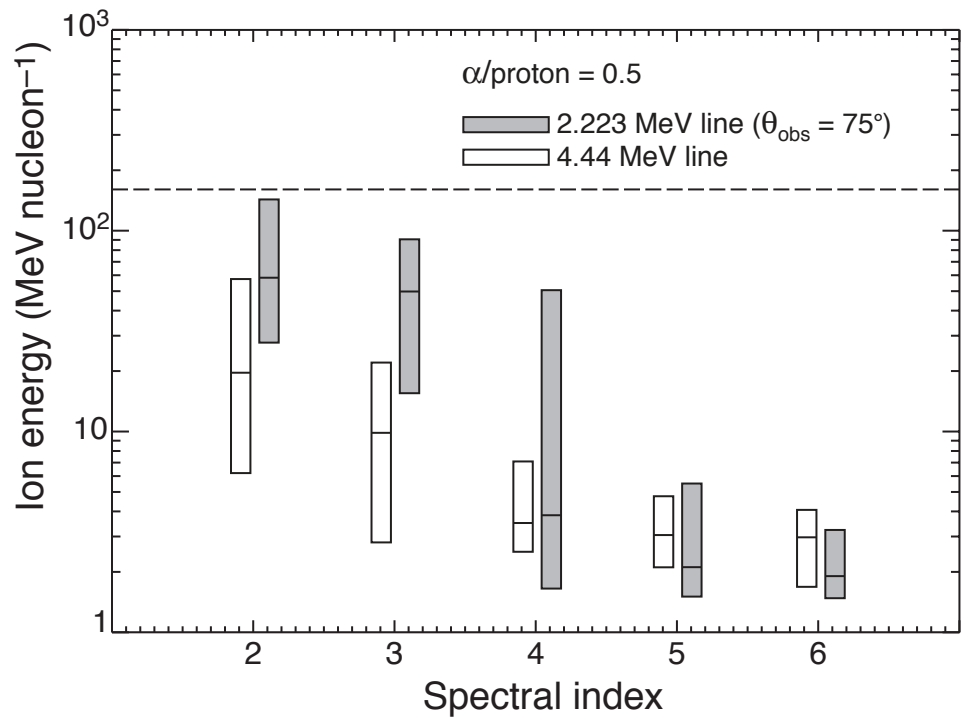

Data Analysis of the 2003 October 28 Flare

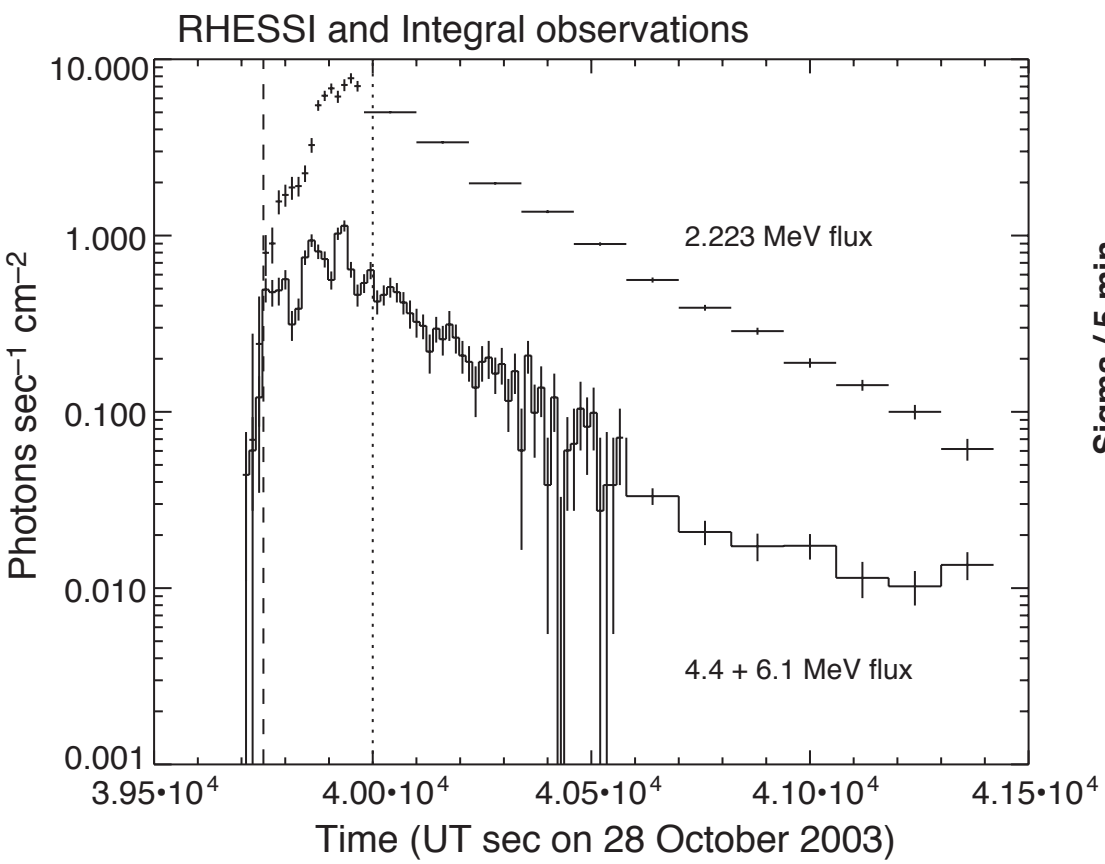

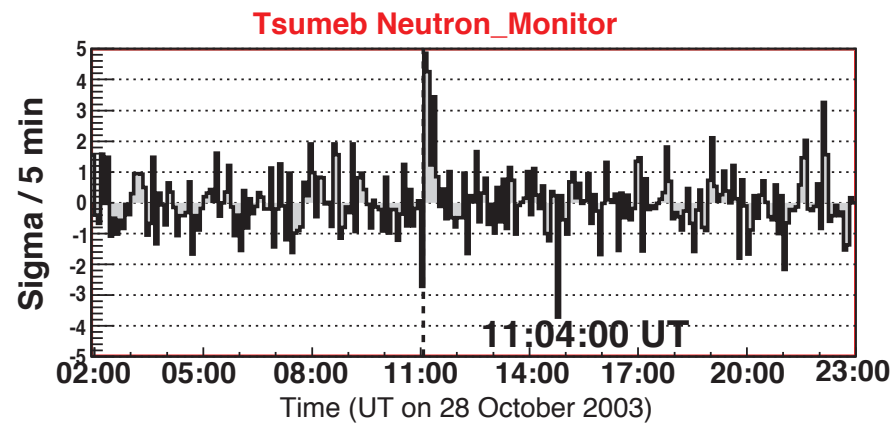

Data Analysis of the 2003 October 28 Flare

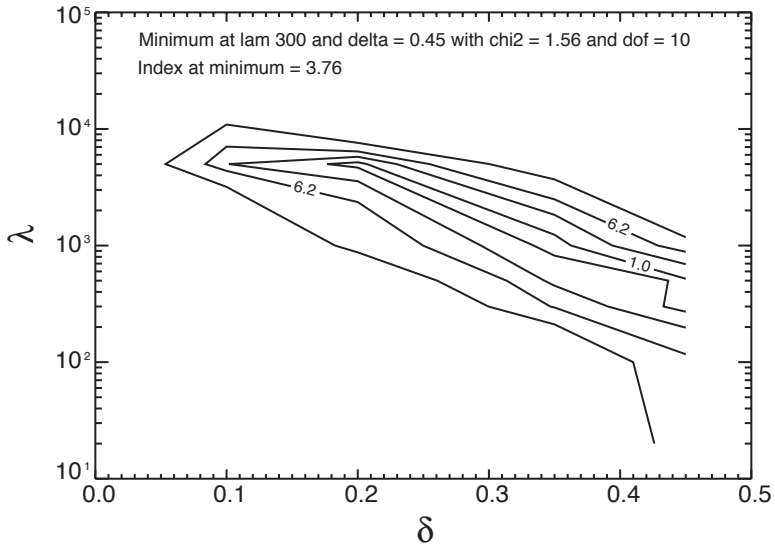

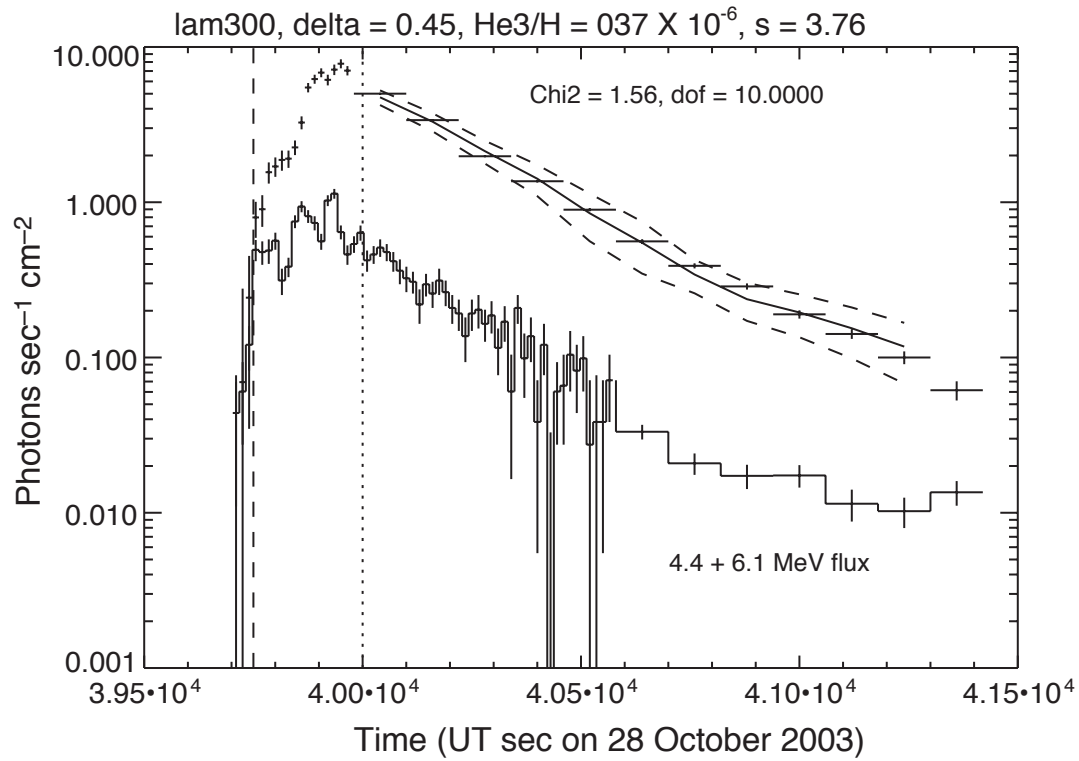

Data Analysis of the 2003 October 28 Flare

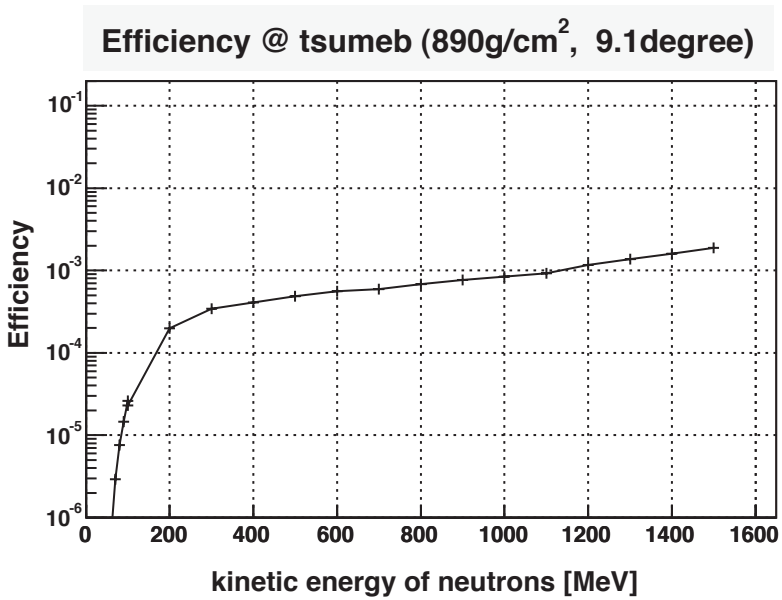

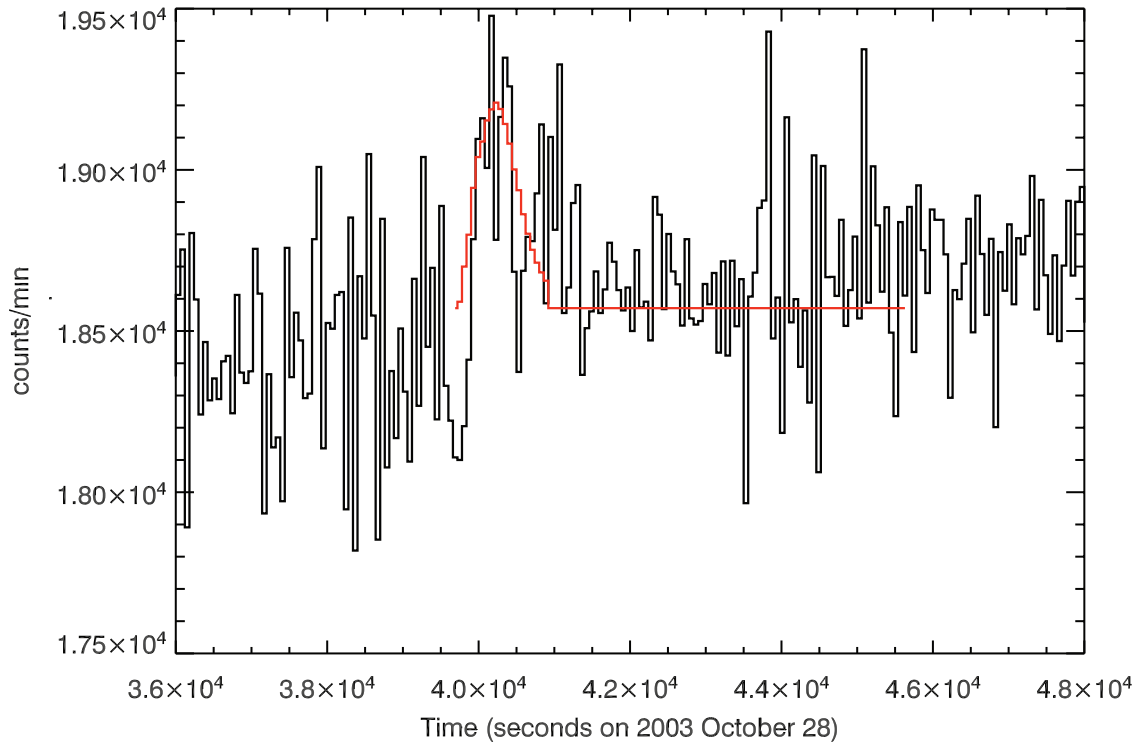

High Energy Solar Flare Data Analysis

The measurable quantities associated with high-energy solar flares can depend in complex ways on the parameters of the transport and interaction model.

Deriving self-consistent and well-constrained values for these parameters with reliable uncertainties can be difficult.

Success requires flare measurements that cover a wide range of the observables and an analysis procedure that takes best advantage of their different parameter dependences.

If a flare dataset cannot support such a full analysis, care must be taken to estimate the additional systematic uncertainties to account for the effects of parameters that have not been explicitly addressed.